Chapter 3

Functional validation of a mammalian-expressed EBA175 antigen and comparative analysis of its binding to MM and MN forms of human Glycophorin A

3.1 INTRODUCTION

3.1.1 Identification and characterisation of *P. falciparum* EBA175 (*Pf*EBA175).

EBA175 was first identified on the basis of its ability to bind human erythrocytes, which seemed to correlate with invasion efficiency (Camus and Hadley, 1985). *Pf*EBA175 is synthesised as a 190 kDa membrane-spanning protein which is later proteolytically cleaved during erythrocyte invasion to release the 175 kDa extracellular domain, hence its name (Orlandi *et al*., 1990). Much of the earliest characterisation of *Pf*EBA175 was carried out using this soluble 175 kDa fragment of the native protein isolated from parasite culture supernatants.

*Pf*EBA175 is one of the four members of the EBL family known to be expressed at the merozoite stage of the *P. falciparum* life cycle (Section 1.7). The members of the EBL family share a strikingly similar gene structure, and this homology has been used to define six regions, RI-RVI, on their ectodomains (Figure 7 A) (Adams *et al*., 1992). Two of these regions, RII and RVI, both contain conserved cysteine and aromatic amino acid residues (Adams *et al*., 1992). RII was initially identified to mediate erythrocyte binding when truncated segments of the *Pf*EBA175 ectodomain were recombinantly expressed on the surface of monkey COS cells and tested for rosetting of erythrocytes (Sim *et al*., 1994). The structure of *Pf*EBA175 RII, which comprises two DBL domains in tandem (F1 and F2), was elucidated by X-ray crystallography to be dimeric, with the constituent monomers interacting in a parallel, handshake arrangement (Figure 7 B) (Tolia *et al*., 2005). The carboxyl-terminal RVI of the *Pf*EBA175 ectodomain is proposed to mediate the trafficking of the protein to micronemes, via interactions with components of the parasite protein-sorting machinery (Gilberger *et al*., 2003). The X-ray crystal structure of this region has revealed the presence of a disulphide-bridged four-helix bundle

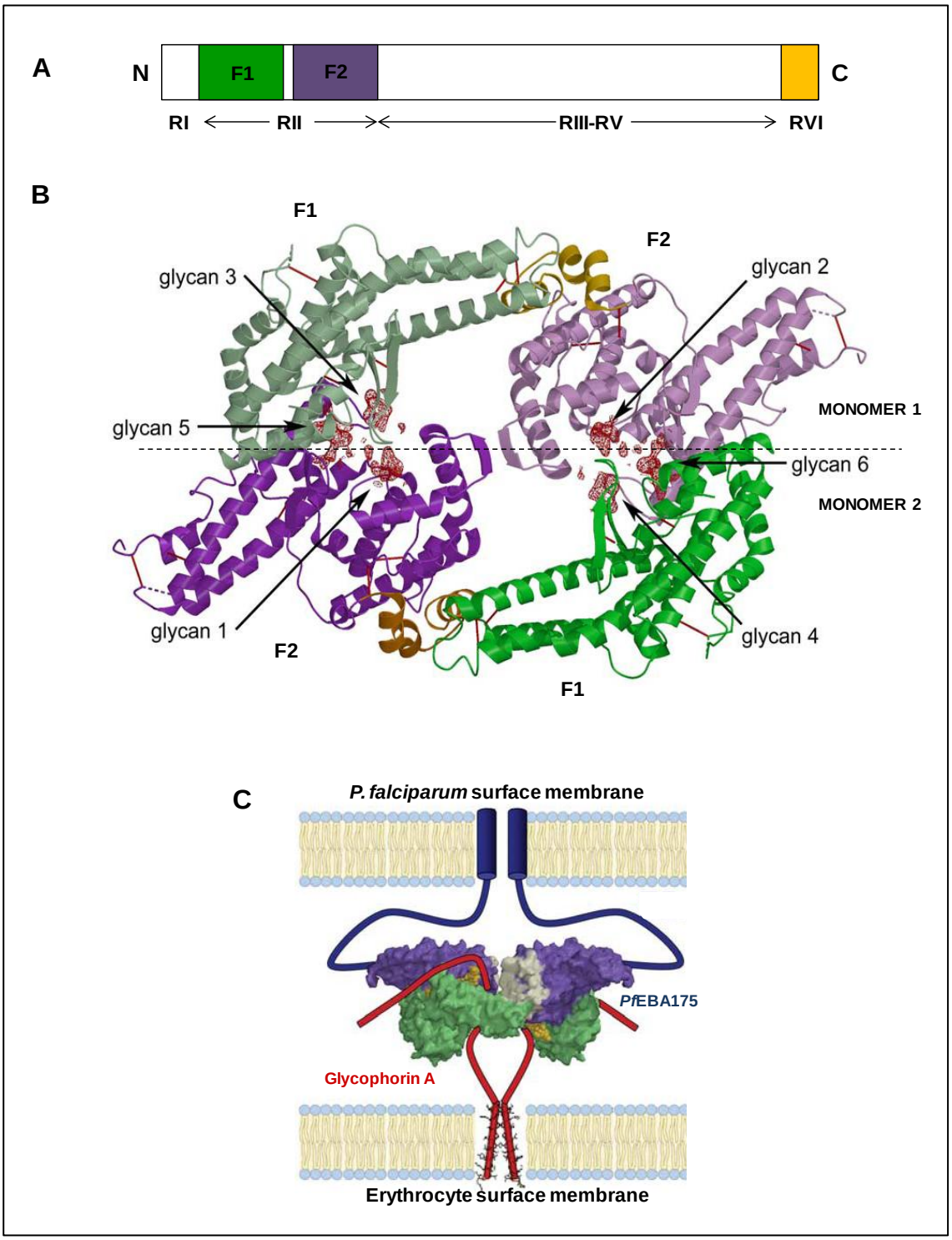
A
N
F1
F2
C
RI
RII
RIII-RV
RVI
B
F1
F2
glycan 3
glycan 2
glycan 5
MONOMER 1
glycan 6
MONOMER 2
glycan 1
F2
glycan 4
F1
C
P. falciparum surface membrane
PfEBA175
Glycophorin A
Erythrocyte surface membrane

Figure 7. *Pf*EBA175 RII: **structure and mode of binding. A)** Schematic of the extracellular domain of *Pf*EBA175 with the six regions of homology (RI-RVI) indicated. The N-terminal RII, which binds to erythrocytes, is rich in cysteine and contains two tandem DBP domains, F1 and F2. **B)** A ribbon representation of the *Pf*EBA175 RII dimer after co-crystallisation with the substrate analogue, α-2, 3-sialyllactose. In the dimer, the two *Pf*EBA175 RII monomers interact in a parallel, handshake arrangement with the F1 domain of one interacting with the F2 domain of the other and *vice versa*. The two monomers are shaded in different intensities in the schematic. The F1 domains are indicated in green and the F2 domains in purple. There are six putative glycan binding sites in the dimer, all located at the interface between the two monomers. Four of the sites are contained within two channels that span the dimer and the other two are found in a deep groove with restricted access from the top surface of the dimer. **C)** Schematic representing the 'ligand-induced dimerisation' model for the *Pf*EBA175-Glycophorin A interaction. This model proposes that free *Pf*EBA175 is predominantly monomeric and that dimerisation occurs upon receptor engagement. (Schematics **B** and **C** were adapted from Tolia *et al.*, 2005).

related to the KIX domain of the CREB-binding protein, which may be involved in such interactions (Withers-Martinez *et al*., 2008).

3.1.2 Interaction of *Pf*EBA175 with the erythrocyte receptor, Glycophorin A.

The *Pf*EBA175 receptor, Glycophorin A, is the most abundant integral membrane protein on the human erythrocyte surface with about 8 x 10^5 copies per cell (Auffray, 2001). It is a type I transmembrane protein which forms homodimers via reversible associations between the hydrophobic membrane-spanning domains (Mackenzie *et al*., 1997). The 70-amino acid extracellular domain of the protein contains the M and N blood group antigens, with the M phenotype characterised by Ser-1 and Gly-5 and the N phenotype by Leu-1 and Glu-5 (Figure 8 A) (Chasis & Mohandas, 1992). The M and N alleles are co-dominant, therefore, heterozygous individuals who carry both alleles, express the M as well as the N form of Glycophorin A, giving rise to the MN blood type. Homozygous individuals who express either the M or the N form of this erythrocyte receptor are of the MM or the NN blood type, respectively. This domain is also heavily sialylated, with 15 O-linked oligosaccharides and 1 N-linked glycan carrying terminal sialic acid (also called N-acetyl neuraminic acid, Neu5Ac) residues (Figure 8) (Tomita & Marchesi, 1975). The Neu5Ac (α-2,3) Gal sequence of the O-linked oligosaccharides has been shown to be essential for the recognition of Glycophorin A by *Pf*EBA175 (Figure 8 B) (Orlandi *et al*., 1992). Co-crystallisation of *Pf*EBA175RII with a structural analogue of this oligosaccharide, α-2,3-sialyllactose, has revealed six putative glycan binding sites at the dimer interface of the parasite protein, with four of the sites located within two channels that span the dimer and another two in a deep groove accessible only through a cavity at the top of the dimer (Figure 7 B) (Tolia *et al*., 2005). Interestingly, the F2 domains of the monomers contributed 75%

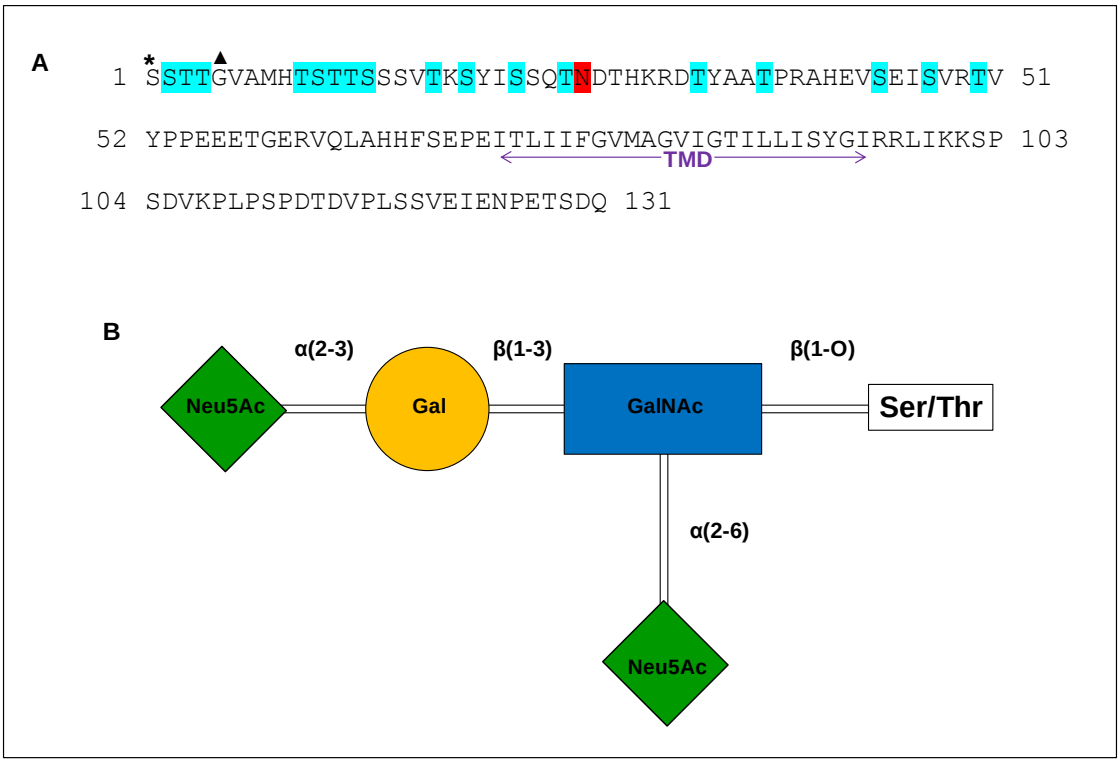

Figure 8. Human Glycophorin A: primary sequence with annotated features. A) Amino acid sequence of mature Glycophorin A (UniProtKB/Swiss-Prot Accession number: P02724), with the potential O-glycosylation sites in the extracellular domain shaded in blue and the N-glycosylation site in red. The given sequence is that of the M antigen. The N antigen of Glycophorin A contains a leucine at position 1 (*) and a glutamate at position 5 (▲). **B)** A schematic diagram of the predominant form of the O-linked tetrasaccharides on Glycophorin A. Neu5Ac-N-acetyl neuraminic acid, Gal-galactose, GalNAc-N-acetylgalactosamine. The glycosidic linkages of the sugar moieties are also indicated.

of the residues in contact with the glycans in the crystal structure, supporting the previous observation of F2 binding to erythrocytes in the absence of F1 (Sim *et al*., 1994; Tolia *et al*., 2005).

Based on the locations of the glycan binding sites in the *Pf*EBA175 RII crystal structure and the predominance of the monomeric form of *Pf*EBA175 RII in solution, Tolia *et al.* (2005) have proposed a ligand-induced dimerisation model for the erythrocyte binding of EBA175, with monomeric EBA175 assembling into a dimer around the dimeric extracellular region of Glycophorin A during invasion (Figure 7 C). This model is also consistent with recent structural studies investigating the mode of binding of the *P. vivax* orthologue DBP RII to its sulfotyrosine-carrying receptor, DARC (Batchelor *et al*., 2012).

3.1.3 *Pf*EBA 175 is an important vaccine candidate.

Some strains of *P. falciparum* such as FVO, Dd2 and MCamp are dependent on the presence of sialic acid on erythrocytes for invasion, whereas others including 3D7, HB3 and 7G8 are capable of invading neuraminidase-treated (i.e. sialic acid-depleted) erythrocytes with relatively high efficiency *in vitro* (Jiang *et al*., 2011). The differential requirement for sialic acid is proposed to reflect the usage of alternative merozoite ligand-erythrocyte receptor pairs for invasion by the various *P. falciparum* strains (Jiang *et al*., 2011; Narum *et al*., 2000; Zhang & Pan, 2005).

Although the interaction between *Pf*EBA175 and Glycophorin A is dependent on the erythrocyte receptor being sialylated, antibodies raised against *Pf*EBA175 RII have been shown to inhibit erythrocyte invasion by both sialic acid-dependent and independent strains of *P. falciparum in vitro* (Narum *et al*., 2000), presumably because *Pf*EBA175 is still functional in both types of strains. This hypothesis is supported by genetic data, where deletion of *Pf*EBA175 in 3D7, a sialic acid-independent stain, results in a shift in the invasion pathways (Duraisingh *et al*., 2003).

Anti-*Pf*EBA175 RII antibodies block the binding of native *Pf*EBA175 from different strains of *P. falciparum* to Glycophorin A, which is probably how they inhibit invasion (Jiang *et al.*, 2011). Interestingly, antibodies raised against RIII-V of the *Pf*EBA175 extracellular domain can also inhibit invasion, leading to the suggestion that these regions may also play a role in a sialic acid-dependent and/or independent invasion pathway (Lopaticki *et al*., 2011; Narum *et al*., 2000).

Based on the observed inhibition of *P. falciparum* blood-stage growth by antibodies directed against *Pf*EBA175 *in vitro* and the detection of anti-*Pf*EBA175 antibodies in malaria-immune individuals, *Pf*EBA175 is currently in consideration as a potential vaccine candidate against severe malaria (El Sahly *et al.,* 2010). The large size of the extracellular domain of *Pf*EBA175 is a technical hurdle for its successful expression as a recombinant protein in heterologous systems, hence, most *in vitro* studies for characterising this protein and assessing its suitability as a vaccine candidate have been conducted with RII, as a substitute. *Pf*EBA175 RII aggregates in insoluble inclusion bodies when over-expressed in *E. coli*, but is soluble and functionally active when produced in insect cells from baculoviral vectors or in the yeast, *Pichia pastoris* (El Sahly *et al*., 2010; Pandey *et al*., 2002; Ockenhouse *et al*., 2001). Antibodies raised against such recombinantly expressed-*Pf*EBA175 RII from one strain of *P. falciparum* have been shown to inhibit invasion by multiple other strains (Jiang *et al*., 2011). However, the level of inhibition observed is at most ~ 60%, suggesting that *Pf*EBA175 RII might not be very efficacious as a vaccine on its own (Narum *et al*., 2000).

3.1.4 Work described in the chapter

Native *Pf*EBA175 is released into *P. falciparum* culture supernatants as the 175 kDa full-length ectodomain fragment. Biochemical investigations of the *Pf*EBA175-Glycophorin A interaction, however, have mainly been performed using the much shorter *Pf*EBA175 RII fragment, as the

production of the full-length ectodomain (*Pf*EBA175 FL) in soluble recombinant form was not feasible in the traditional heterologous expression systems. There is a possibility of extracellular regions of *Pf*EBA175 outside of RII playing a yet unidentified role in erythrocyte invasion. *Pf*EBA175 FL is therefore potentially a better vaccine candidate than *Pf*EBA175 RII on its own. In this study, a soluble *Pf*EBA175 FL antigen, produced using a codon-optimised expression construct in mammalian cells, was extensively characterised using biochemical methods to confirm functional similarity to native *Pf*EBA175 isolated from parasite cultures and to gain mechanistic insight into its interaction with Glycophorin A. The binding of recombinant *Pf*EBA175 FL to human erythrocytes, native human Glycophorin A (purified from MM and MN erythrocytes) and a recombinantly-expressed full-length ectodomain of human Glycophorin A, was analysed.

3.2 RESULTS

3.2.1 *Pf*EBA175 FL was expressed as a soluble fusion protein and immunologically characterised.

The coding sequence of the full-length ectodomain of *Pf*EBA175 was derived from the 3D7 isolate of *P. falciparum* (MAL7P1.176) and codon optimised by gene synthesis for expression in the suspension culture-adapted human cell line, HEK293E (Section 2.1.1). As *P. falciparum* proteins are not known to be glycosylated (Gowda & Davidson, 1999), the potential N-linked glycosylation sites on *Pf*EBA175 were systematically removed during gene synthesis to prevent inappropriate addition of glycans in the human secretory pathway. The full-length ectodomain of *Pf*EBA175 (*Pf*EBA175 FL) was produced as a fusion protein with a mouse signal peptide to ensure secretion into the cell culture medium and with two carboxyl-terminal fusion partners: Cd4 and an enzymatically biotinylatable peptide tag (Section 2.1.1 and Figure 5). Expression of

biotinylated *Pf*EBA175 FL at the expected size of 185.7 kDa was confirmed by western blotting (Figure 9 A). Biotinylated Cd4, of 25 kDa, was used as a positive control in the blot.

*Pf*EBA175 FL was quantified relative to the highly expressed protein Cd4 (typical yield > 1 mg/ml) by ELISA as described in section 2.2.3. The ELISA results shown indicate an approximately 16-fold lower expression of *Pf*EBA175 FL (Figure 9 B). However, the levels of expression of both Cd4 and *Pf*EBA175 FL were observed to vary quite significantly from one batch of transfections to another (data not shown), most likely due to differences in transfection efficiency.

To determine whether the recombinant *Pf*EBA175 FL was correctly folded, its recognition by two mouse monoclonal antibodies, R217 and R218 were tested. R217 and R218, raised against a *Pf*EBA175 RII antigen produced using a baculovirus expression system, are known to bind to non-linear, heat-labile epitopes within EBA175 RII (Sim *et al*., 2011). *Pf*EBA175 FL was recognised by both R217 and R218 and heat-treatment of *Pf*EBA175 FL was observed to significantly reduce this immuno-reactivity, suggesting that the R217 and R218 epitopes are correctly folded in the mammalian-expressed full-length ectodomain. No significant binding of R217 and R218 to Cd4, the negative control, was observed (Figure 9 C).

Another mouse monoclonal antibody, raised against a yeast-derived *Pf*EBA175 RVI antigen (O'Donnell *et al.*, 2006) was also tested against *Pf*EBA175 FL by ELISA as described previously (Figure 9 D). This antibody showed similar binding to both untreated and heat-treated samples of *Pf*EBA175 FL, suggesting that it recognises a non-heat labile, linear epitope within EBA175 RVI. No binding of this antibody was seen to Cd4, the negative control.

All available anti-EBA175 monoclonals that recognise heat-labile epitopes therefore indicate that *Pf*EBA175 FL is correctly folded.

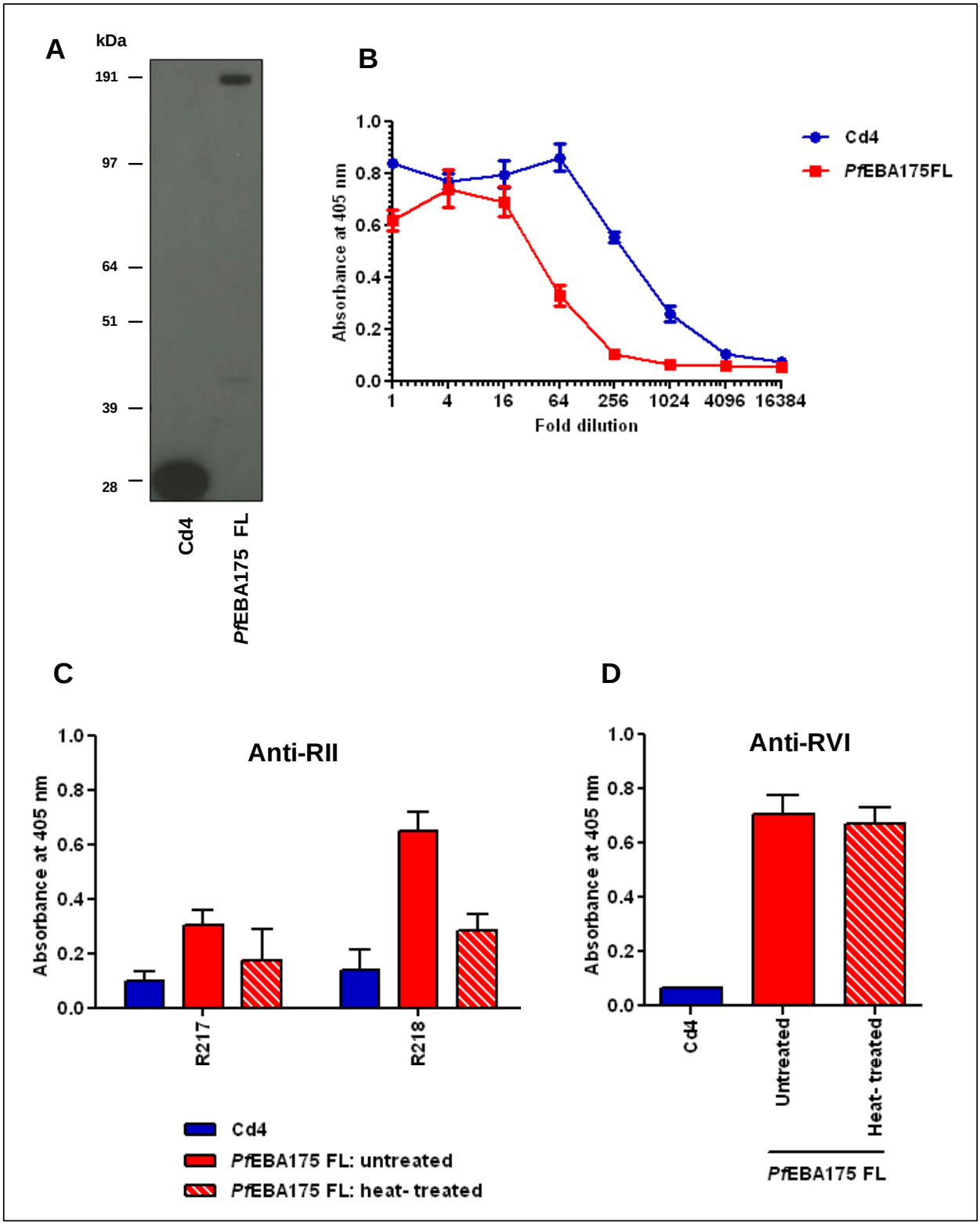
A
kDa
191
97
64
51
39
28
Cd4
PfEBA175 FL
B
Absorbance at 405 nm
Fold dilution
Cd4
PfEBA175FL
C
Anti-RII
Absorbance at 405 nm
R217
R218
Cd4
PfEBA175 FL: untreated
PfEBA175 FL: heat- treated
D
Anti-RVI
Absorbance at 405 nm
Cd4
Untreated
Heat- treated
PfEBA175 FL

Figure 9. Recombinant *Pf*EBA175 FL was expressed at the expected size and immunologically active. *Pf*EBA175 FL was expressed in the soluble form with C-terminal Cd4 and biotin tags using the HEK293E expression system. **A)** A western blot of *Pf*EBA175 FL (185.7 kDa) and monobiotinylated Cd4 (25 kDa), performed using HRP-conjugated extravidin as the probe. **B)** Quantitation of *Pf*EBA175 FL relative to Cd4 by ELISA. The anti-Cd4 mouse monoclonal OX68, was used as the primary antibody. **C)** and **D)** Recognition of untreated and heat-treated *Pf*EBA175 FL by two mouse monoclonals, R217 and R218, raised against a baculovirus-derived *Pf*EBA175 RII antigen **(C)** and a mouse monoclonal, raised against a yeast-expressed *Pf*EBA175 RVI antigen **(D)**. Binding of these monoclonals was also detected by ELISA. Cd4 was used as the negative control in the assays. All ELISAs were performed on streptavidin-coated plates, using an alkaline phosphatase-conjugated anti-mouse antibody as the secondary. Alkaline phosphatase activity was quantified by the turnover of the colorimetric substrate, *p*-nitrophenyl phosphate, measured as an increase in absorbance at 405 nm. The graphically presented data indicate mean ± standard deviation; n=3.

3.2.2 Recombinant *Pf*EBA175 FL showed Glycophorin A-dependent binding to human erythrocytes.

To determine whether the mammalian-expressed *Pf*EBA175 FL is functionally active, a flow cytometry-based, quantitative assay was developed to investigate its binding to Glycophorin A on human erythrocytes.

Interactions between cell surface proteins are generally of very low affinity. Therefore, to enable detection of its interaction with Glycophorin A, highly-avid, multimeric arrays of *Pf*EBA175 FL were first generated by direct immobilisation of the biotinylated protein on streptavidin-coated Nile red beads. To monitor the process of immobilising *Pf*EBA175 FL on beads and to determine the least amount of protein necessary for full saturation of a set number of beads, ELISA assays were performed on 2-fold serially-diluted samples of *Pf*EBA175 FL with and without prior incubation with beads (Figure 10 A). This assessment was deemed necessary, because non-saturation of beads with *Pf*EBA175 FL could decrease the avidity of the resulting arrays, whereas the presence of excess amounts of free (non-bead bound) *Pf*EBA175 FL could potentially act in an inhibitory manner against the binding of the arrays to erythrocytes. Similar bead arrays were also constructed with Cd4, to use as negative controls in the erythrocyte binding assays.

The protein-coated bead arrays generated were then incubated with human erythrocytes and analysed by flow cytometry. Erythrocytes incubated with *Pf*EBA175 FL-coated beads were observed to have higher forward scatter (FSC) and side scatter (SSC) values on average than those incubated with Cd4-coated beads (FSC and SSC values are directly proportional to the size and granularity of the cells sampled, respectively) (Figure 10 B). Incubation with *Pf*EBA175 FL-coated beads also caused a large upwards shift in the fluorescence intensity (~ 10^3 difference in

median fluorescence) of the erythrocyte population at the Nile red emission wavelength relative to Cd4-coated beads (Figures 10 C and D). These observations together suggest that *Pf*EBA175 FL-coated beads were binding to human erythrocytes. The specificity of the detected association was then probed using treatments known to interfere with the *Pf*EBA175-Glycophorin A interaction, either enzymatic (pre-treatment of erythrocytes with trypsin, chymotrypsin and neuraminidase) or immunological (pre-incubation of erythrocytes with an anti-Glycophorin A monoclonal antibody), prior to being presented with *Pf*EBA175 FL-coated beads.

Glycophorin A has previously been demonstrated to be sensitive to treatment with the protease trypsin but not chymotrypsin (Camus & Hadley, 1985). Human erythrocytes were therefore pre-treated with 0.25, 0.5 and 1 mg/ml of trypsin and chymotrypsin prior to incubation with the protein-coated bead arrays. Pre-treatment of erythrocytes with trypsin reduced the binding of *Pf*EBA175 FL-coated beads in a concentration-dependent manner (Figure 11 A). By contrast, the binding of *Pf*EBA175-coated beads to erythrocytes was not significantly affected by pre-treatment with chymotrypsin (Figure 11 B).

The binding of *Pf*EBA175 FL-coated beads was completely inhibited by pre-treatment of erythrocytes with the *Vibrio cholerae* neuraminidase, which preferentially cleaves α (2→ 3) linked sialic acids of O-glycans that are necessary for the *Pf*EBA175-Glycophorin A interaction (Figure 11 C, Section 3.1.1). The enzymatic susceptibility profile of the *Pf*EBA175 FL-human erythrocyte interaction therefore matches the profile of the *Pf*EBA175-Glycophorin A interaction.

To gain more direct confirmation of specificity, the possibility of inhibiting the association of *Pf*EBA175 FL with human erythrocytes using anti-Glycophorin A monoclonals was tested. As a preliminary step two anti-Glycophorin A monoclonal antibodies, 11E4B7 and BRIC256, were

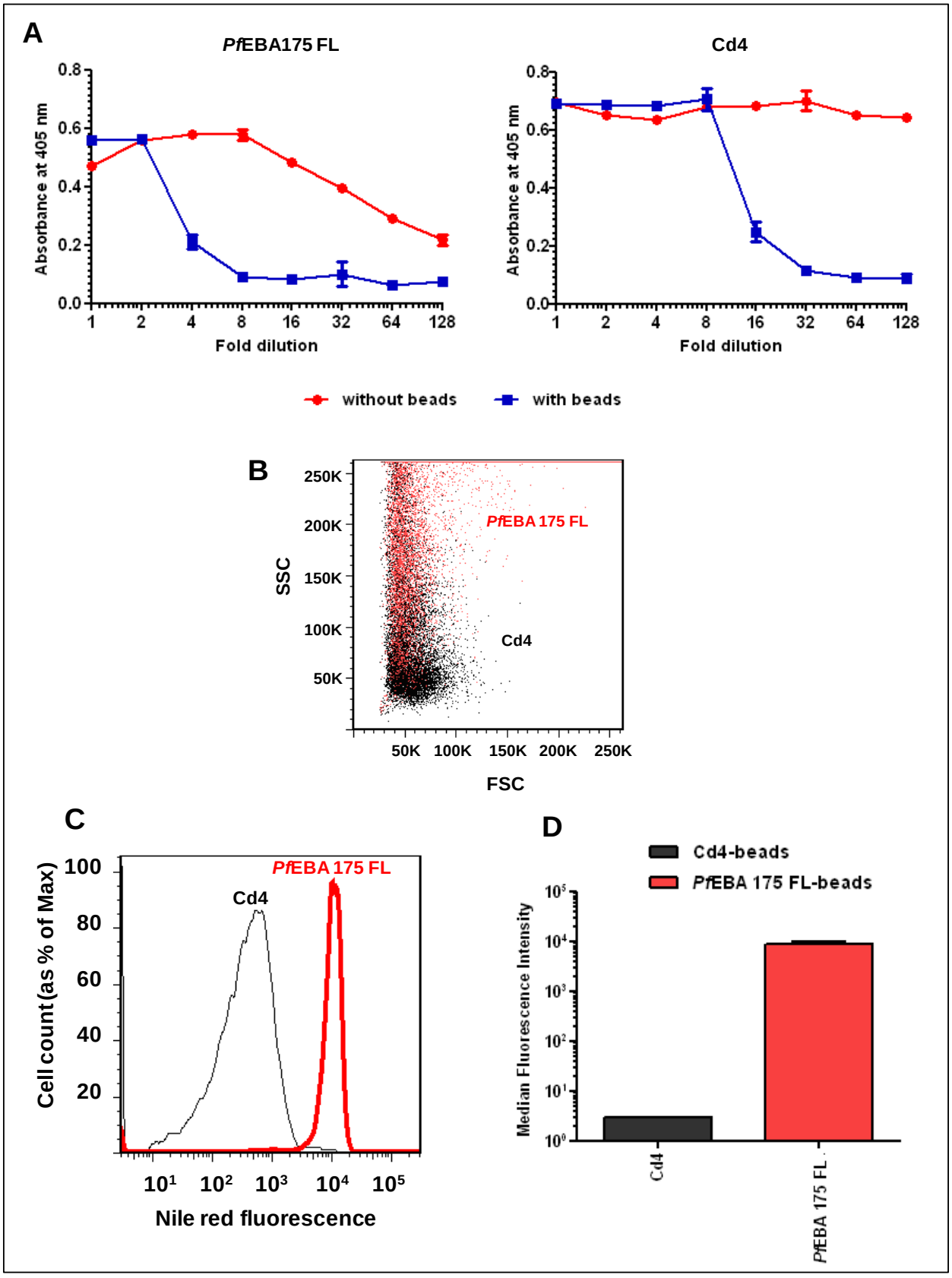
A
PfEBA175 FL
Cd4
Absorbance at 405 nm
Fold dilution
without beads
with beads
B
PfEBA 175 FL
Cd4
SSC
FSC
C
PfEBA 175 FL
Cd4
Cell count (as % of Max)
Nile red fluorescence
D
Cd4-beads
PfEBA 175 FL-beads
Median Fluorescence Intensity
Cd4
PfEBA 175 FL

0

Figure 10. Recombinant *Pf*EBA175 FL showed binding to human erythrocytes. To monitor the binding of *Pf*EBA175 FL to human erythrocytes, multimeric arrays of the protein were generated by immobilising on streptavidin-coated Nile red beads. Erythrocytes were incubated with these arrays for 1 h at 4°C before analysis by flow cytometry. Cd4-coated beads were used as the negative control in these erythrocyte binding assays. **A)** To determine the minimum amount of *Pf*EBA175 FL and Cd4 necessary for complete saturation of a set number of streptavidin-coated Nile red beads, ELISAs were performed on 2-fold serial dilutions of the proteins, with and without pre-incubation with beads. The ELISAs were carried out on a streptavidin-coated plate, using OX68 as the primary antibody and an alkaline phosphatase-conjugated anti-mouse antibody as the secondary. Data is shown as mean ± standard deviation; *n*=3. Based on the ELISA results, *Pf*EBA175 FL and Cd4 were used at dilutions of 4-fold and 16-fold respectively, for coating the fluorescent beads, which were then incubated with erythrocytes. **B)** A dot-plot of the FSC (α size) and SSC (α granularity) parameters of the erythrocyte populations as estimated by flow cytometry. **C)** A histogram of the fluorescence intensity of the erythrocyte populations at the Nile red emission wavelength, as a function of cell count. **D)** Representation of the median fluorescence intensity of erythrocyte populations at the Nile red emission wavelength. Each bar indicates mean ± standard deviation; *n*=3. In **B**, **C** and **D**, erythrocytes incubated with *Pf*EBA175 FL-coated beads are indicated in red and those incubated with Cd4-coated beads in black.

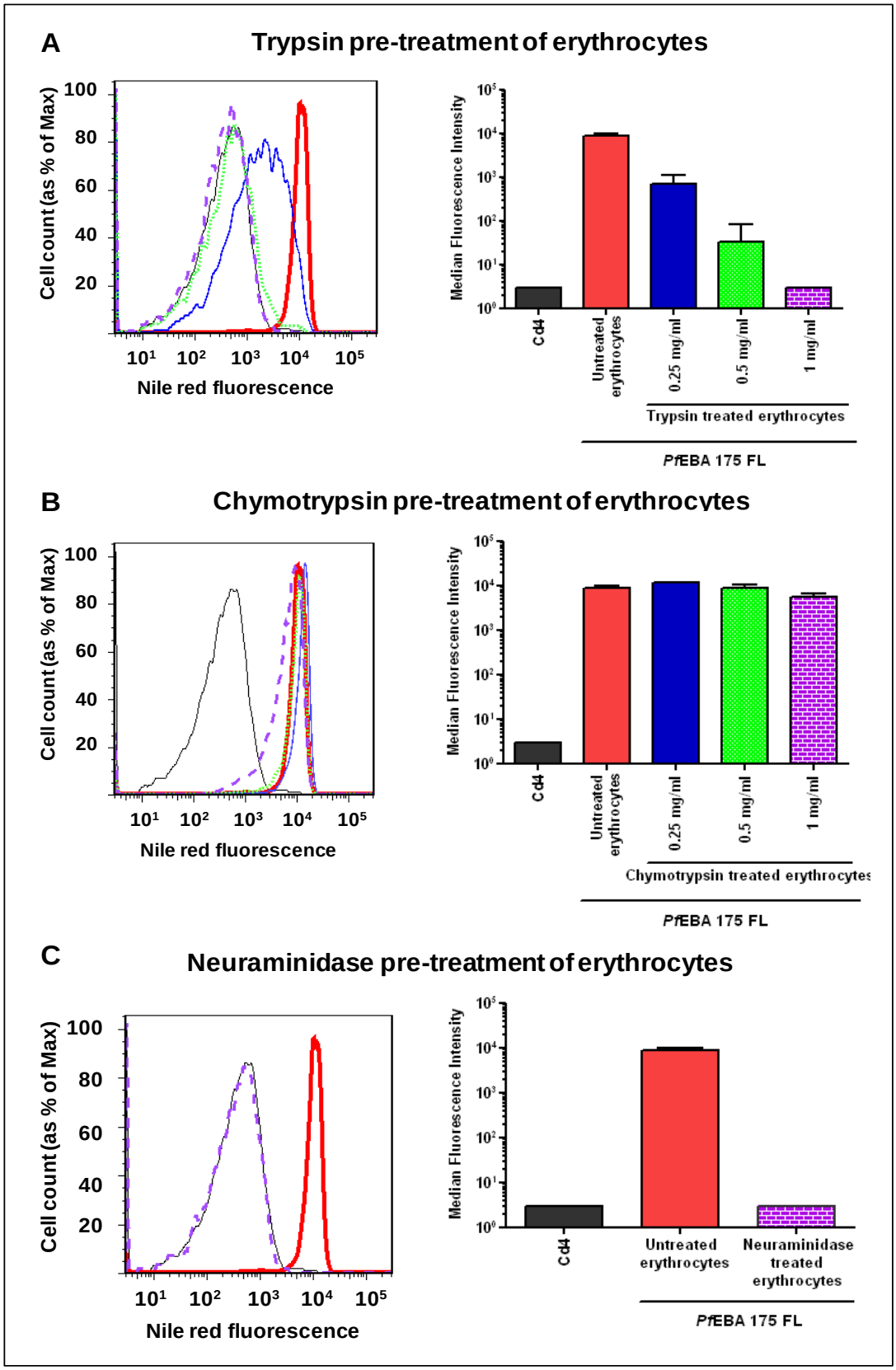
A
Trypsin pre-treatment of erythrocytes
Cell count (as % of Max)
Nile red fluorescence
Median Fluorescence Intensity
Cd4
Untreated erythrocytes
0.25 mg/ml
0.5 mg/ml
1 mg/ml
Trypsin treated erythrocytes
PfEBA 175 FL
B
Chymotrypsin pre-treatment of erythrocytes
Cell count (as % of Max)
Nile red fluorescence
Median Fluorescence Intensity
Cd4
Untreated erythrocytes
0.25 mg/ml
0.5 mg/ml
1 mg/ml
Chymotrypsin treated erythrocytes
PfEBA 175 FL
C
Neuraminidase pre-treatment of erythrocytes
Cell count (as % of Max)
Nile red fluorescence
Median Fluorescence Intensity
Cd4
Untreated erythrocytes
Neuraminidase treated erythrocytes
PfEBA 175 FL

Figure 11. The binding of *Pf*EBA175 FL to human erythrocytes was sensitive to treatment with trypsin and neuraminidase, but not chymotrypsin. Human erythrocytes were pre-treated with the enzymes, trypsin **(A)**, chymotrypsin **(B)** and neuraminidase **(C)** prior to incubation with *Pf*EBA175 FL-coated beads and analysis by flow cytometry. The histograms and the bar charts represent the fluorescence intensity of the erythrocyte populations at the Nile red emission wavelength. Untreated erythrocytes incubated with *Pf*EBA175 FL-coated beads (positive control) and Cd4-coated beads (negative control), are indicated in red and black respectively. **A)** Erythrocytes pre-treated with 0.25, 0.5 and 1 mg/ml of trypsin are represented in blue, green and purple respectively. **B)** Erythrocytes pre-treated with 0.25, 0.5 and 1 mg/ml of chymotrypsin are indicated in blue, green and purple respectively. **C)** Erythrocytes pre-treated with 100 mU/ml of neuraminidase are represented in purple. All enzymatic pre-treatments were carried out for 1 h at 37°C. The bar charts show mean ± standard deviation; n=3.

first tested for binding to human erythrocytes. 11E4B7 and BRIC256 have been raised using human erythrocytes and full-length native human Glycophorin A as immunogens, respectively. At the concentration used (0.5 µg of antibody/10^6 cells), 11E4B7 caused erythrocytes to aggregate, BRIC256 however showed clear binding to erythrocytes without causing cell aggregation (Figure 12 A). Pre-incubation of erythrocytes with BRIC256, significantly decreased the binding of *Pf*EBA175 FL-coated beads, confirming the Glycophorin A-dependency of the association of *Pf*EBA175 FL-coated beads with human erythrocytes (Figure 12 B).

3.2.3 Recombinant *Pf*EBA175 FL showed binding to native human Glycophorin A in a sialic acid-dependent manner.

As a second independent assay for validating the activity of *Pf*EBA175 FL, its binding to native Glycophorin A extracted from human erythrocyte membranes was tested using an ELISA-based method adapted from AVEXIS (Section 2.5.2). Glycophorin A from both MM and MN blood types were included as well as an asialylated form Glycophorin A from the MN blood type.

As the 'Neu5Ac (α-2,3) Gal' sequence of the O-linked tetrasaccharides of Glycophorin A is known to be essential for its interaction with *Pf*EBA175 (Section 3.1.1) , the glycan composition of the commercially available native Glycophorin A preparations was first tested by analysing its binding to three lectins with known glycan-binding preferences, *Arachis hypogaea* lectin (recognising non-sialylated Gal (β-1,3) GalNAc), *Sambucus nigra* lectin (recognising terminal Neu5Ac (α-2,6)) and *Maackia amurensis* lectin (recognising terminal Neu5Ac (α-2,3)). The biotinylated lectins were immobilised on streptavidin-coated plates and probed with the native Glycophorin A preparations using an ELISA-based method as described in Section 2.6.1. Native Glycophorin A (both MM and MN forms) seemed to predominantly carry glycans with terminal

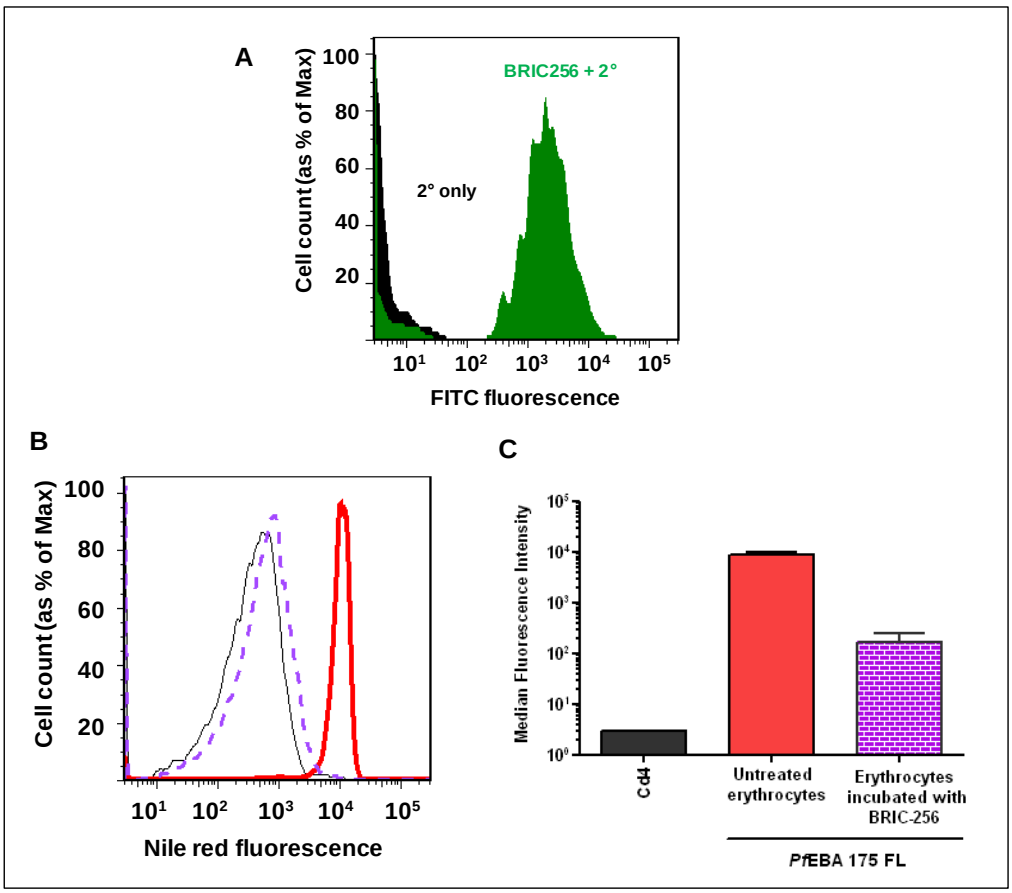

Figure 12. The binding of *Pf*EBA175 FL to human erythrocytes was significantly reduced by pre-incubation of cells with an anti-Glycophorin A monoclonal (BRIC256). Human erythrocytes were pre-treated with BRIC256 prior to incubation with *Pf*EBA175 FL-coated beads and analysis by flow cytometry. **A)** A histogram showing the staining of human erythrocytes by BRIC256, detected using a FITC-conjugated anti-mouse secondary (green). Erythrocytes incubated with only the secondary antibody (negative control) are represented in black. **B)** and **C)** Histogram and bar chart of the fluorescence intensity of the erythrocyte populations at the Nile red emission wavelength. Untreated erythrocytes incubated with *Pf*EBA175 FL-coated beads (positive control) and Cd4-coated beads (negative control), are indicated in red and black respectively. Erythrocytes pre-treated with BRIC256 (0.5 µg /10^6 cells) for 1 h at room temperature prior to incubation with *Pf*EBA175 FL-coated beads, are represented in purple. The bar chart shows mean ± standard deviation; *n*=3.

Neu5Ac (α-2,3), whereas the asialylated Glycophorin A preparation mainly contained non-sialylated Gal (β-1,3) GalNAc (Figure 13 A).

The native Glycophorin A preparations were then biotinylated *in vitro* to enable immobilisation on streptavidin-coated plates, for testing their binding to *Pf*EBA175 FL. The amount of biotinylated protein in each of the three Glycophorin A preparations was quantified relative to each other by ELISA using BRIC256 as the primary antibody (Figure 13 B).

For probing against native Glycophorin A, *Pf*EBA175 FL was expressed as a soluble β-lactamase tagged pentamer, by in-frame fusion with the pentamerisation domain of the rat COMP protein and a β-lactamase enzyme, in addition to the Cd4 tag, as described in Section 2.1.1 (Figure 5). The level of expression of *Pf*EBA175 FL was compared to that of pentameric, β-lactamase tagged Cd4 by monitoring the turnover of the β-lactamase substrate, nitrocefin in a time-course assay (Section 2.2.4). Neat, 2-fold and 4-fold dilutions of the proteins were tested in this manner. The level of expression of *Pf*EBA175 FL was lower than the threshold specified for the AVEXIS assay (i.e. sufficient protein in 20 µl of filtered culture supernatant for complete turnover of 7.5 µg of nitrocefin within 10 min), and so had to be concentrated 5-fold, the results shown for *Pf*EBA175 FL are from the β-lactamase activity assay done after this step (Figure 14 A).

Biotinylated native Glycophorin A preparations, immobilised on a streptavidin-coated plate, were finally probed with normalised *Pf*EBA175 FL and Cd4 'prey' proteins in a 2-fold dilution series. Both MM and MN forms of Glycophorin A showed similar levels of clear, saturable binding to *Pf*EBA175 FL, but not to Cd4 (Figure 14 B). Some slight binding to *Pf*EBA175 FL was also observed with asialylated Glycophorin A, which might have been due to the presence of some sialylated Glycophorin A in the initial protein preparation (Figure 14 B).

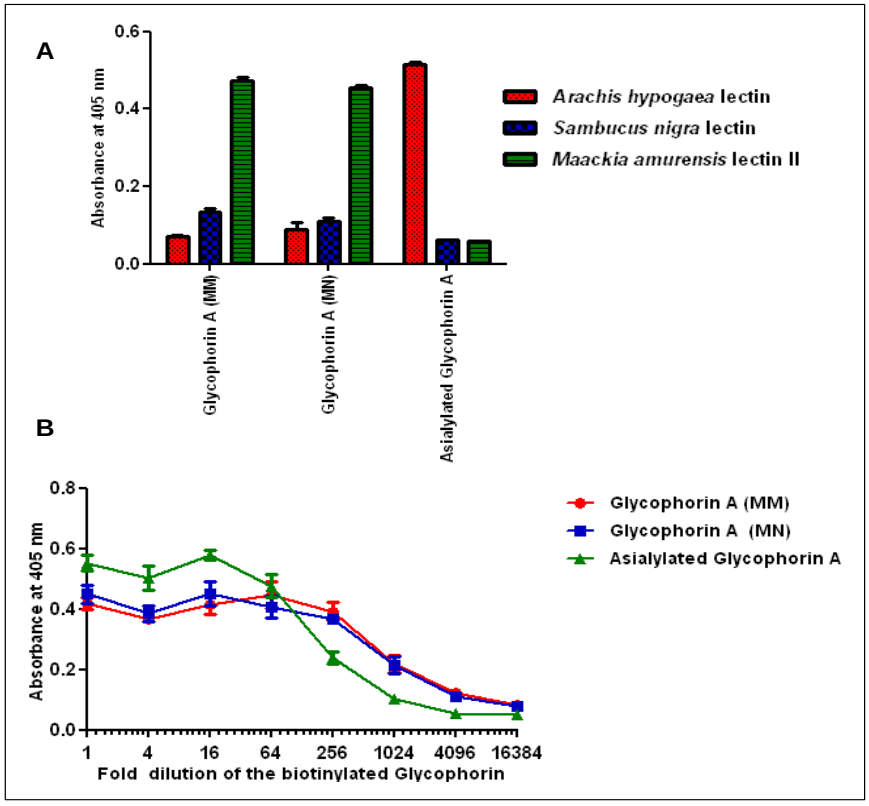

Figure 13. Commercially-available native human Glycophorin A preparations were biochemically characterised. A) Analysis of the glycan composition of the native Glycophorin A preparations, performed by the testing binding to three lectins using an ELISA-based method. The biotinylated lectins were immobilised on a streptavidin coated-plate and incubated with the Glycophorin A preparations (used at 0.02 mg/ml) for 2 h at room temperature. The glycan-binding specificities of the three lectins are as follows: *Arachis hypogaea* lectin (red)- non-sialylated Gal (β-1,3) GalNAc, *Sambucus nigra* lectin (blue)- terminal Neu5Ac (α-2,6) and *Maackia amurensis* lectin (green)- terminal Neu5Ac (α-2,3). **B)** The native Glycophorin A preparations were subsequently biotinylated *in vitro* for use in downstream assays. The amount of biotinylated protein in each of the preparations was normalised against each other by ELISA on a streptavidin-coated plate. In both assays, **A** and **B**, the binding of Glycophorin A was detected by sequential incubation with BRIC256 as the primary antibody and an alkaline phosphatase-conjugated anti-mouse secondary. All data is shown as mean ± standard deviation; *n*=3.

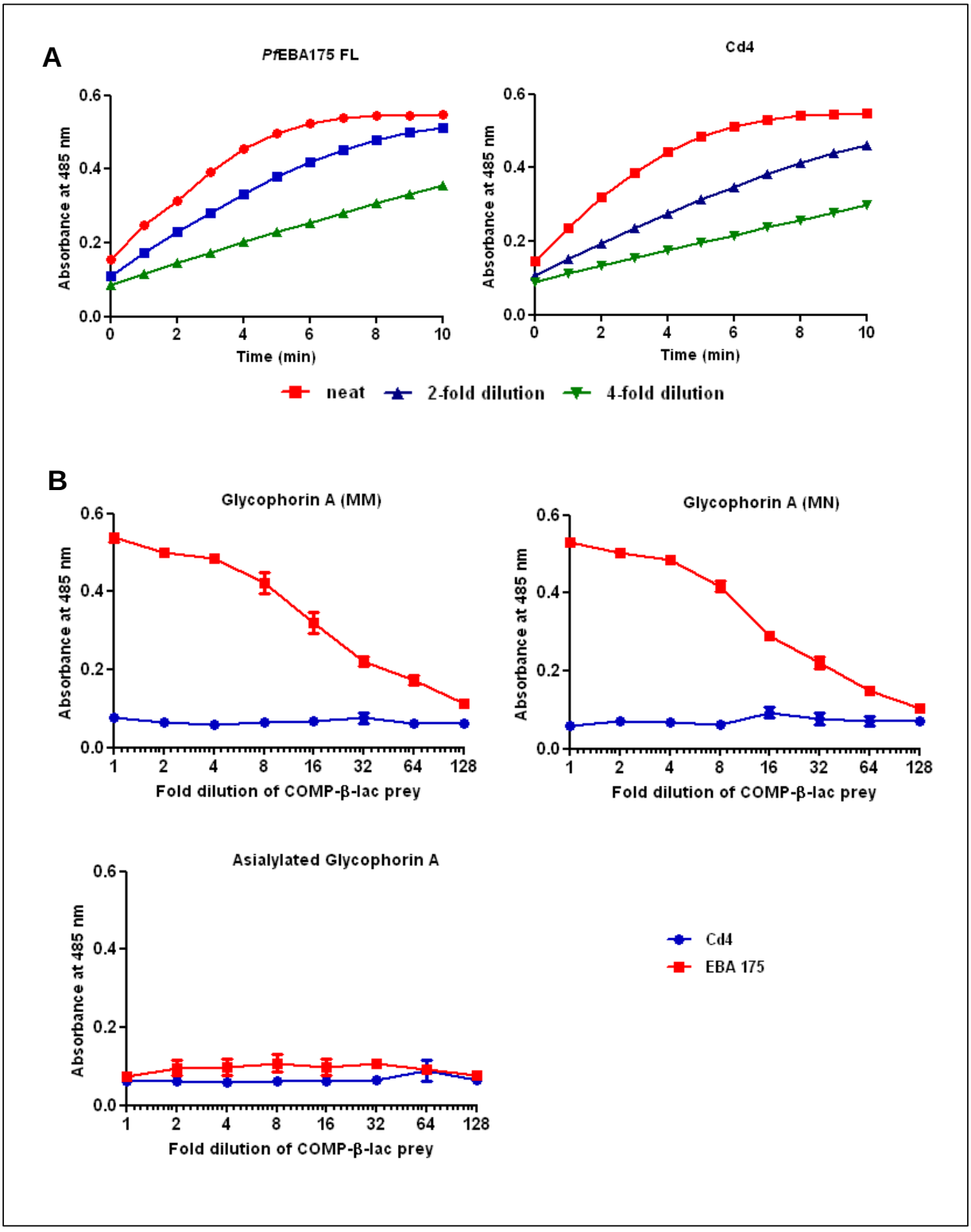
A
PfEBA175 FL
Cd4
Absorbance at 485 nm
Time (min)
neat
2-fold dilution
4-fold dilution
B
Glycophorin A (MM)
Glycophorin A (MN)
Asialylated Glycophorin A
Fold dilution of COMP-β-lac prey
Cd4
EBA 175

Figure 14. Recombinant *Pf*EBA175 FL showed sialic acid-dependent binding to native human Glycophorin A. *Pf*EBA175 FL, expressed as a soluble β-lactamase tagged pentamer was tested against the three biotinylated Glycophorin A preparations; sialylated native Glycophorin A of the MM and MN blood types and asialylated Glycophorin A, all immobilised on a streptavidin-coated plate. **A)** Prior to testing against Glycophorin A, *Pf*EBA175 FL and Cd4, both expressed in the pentameric form with a β-lactamase tag, were normalised against each other using a time-course assay, monitoring the turnover of the colorimetric β-lactamase substrate, nitrocefin, at an absorbance of 485 nm. **B)** A 2-fold dilution series of *Pf*EBA175 FL was probed against Glycophorin A and binding was detected using nitrocefin. Cd4 was used as the negative control in the assay. The pentameric proteins were incubated with the immobilised Glycophorin A for 2 h at room temperature and the absorbance at 485 nm was measured 1 h after the addition of nitrocefin. COMP- the pentamerisation tag. The data are shown as mean ± standard deviation; *n*=3.

3.2.4 The full-length ectodomain of human Glycophorin A was expressed in soluble recombinant form.

While commercially-available native human Glycophorin A can be used to confirm functionality of *Pf*EBA175 FL, a more detailed biochemical characterisation of the interaction requires recombinantly-expressed Glycophorin A, both because it would be amenable to site-directed mutagenesis and because it could potentially be isolated in much larger quantities with higher levels of purity than the native protein. The full-length ectodomain of human Glycophorin A (NP_002090.4) was therefore expressed in soluble, recombinant form using the HEK293E expression system.

For use in reciprocal AVEXIS assays with *Pf*EBA175 FL, the full-length ectodomain of Glycophorin A was expressed as both a mono-biotinylated 'bait' and as a pentameric β-lactamase tagged 'prey' protein as described above for *Pf*EBA175 FL. Human Glycophorin B (NP_002091.3) was also expressed with the same fusion partners, for use as a negative control in the AVEXIS assays. The proteins were normalised by ELISA (biotinylated proteins) (Figure 15 B) and β-lactamase activity assays (Figure 15 D). To confirm expression at the correct size, biotinylated recombinant Glycophorin A and B were analysed by western blotting using a streptavidin-HRP probe (Figure 15 A). The expected molecular weights of un-glycosylated monomers of recombinant Glycophorin A and B were 32.2 and 28.8 kDa respectively. The migration of these recombinant proteins as broad smears was probably due to the structural heterogeneity of the carbohydrate moieties added on to the protein backbone during glycosylation in the secretory pathway.

To confirm expression of recombinant Glycophorin A in the native conformation, the biotinylated proteins were probed with two anti-Glycophorin A mouse monoclonal antibodies,

11E4B7 and BRIC256, by ELISA (Figure 15 C). Both 11E4B7 and BRIC256 showed higher binding to untreated Glycophorin A than to its heat-treated derivative, suggesting the presence of correctly folded, heat-labile epitopes in the recombinant antigen. No binding of either was observed to the negative control, Glycophorin B. Interestingly 11E4B7 showed significantly greater binding to Glycophorin A than BRIC256 and as both antibodies were used at equivalent amounts, the former likely binds Glycophorin A with much higher affinity, potentially explaining the aggregation-inducing behaviour of 11E4B7 in the erythrocyte-staining experiment described previously in Section 3.2.1.

The glycan composition of the recombinant Glycophorins was analysed by incubation of their pentameric, β-lactamase tagged 'prey' forms with the biotinylated lectins from *Arachis hypogaea, Sambucus nigra* and *Maackia amurensis* as described in Section 2.6.1 (Figure 15 E). Both recombinant Glycophorin A and B, were observed to contain some glycans with terminal Neu5Ac (α-2,3) and Neu5Ac (α-2,6) but seemed to predominantly carry non-sialylated Gal (β-1,3) GalNAc moieties. Cd4, which doesn't contain any O-linked glycosylation sites, was used as the control 'prey' in this assay.

3.2.5 No binding was detected between recombinant human Glycophorin A and *Pf*EBA175 FL using AVEXIS.

The binding of recombinant Glycophorin A to *Pf*EBA175 FL was analysed in reciprocal AVEXIS assays.

When the pentameric, β-lactamase tagged *Pf*EBA175 FL 'prey' was tested against the biotinylated 'bait' form of recombinant Glycophorin A, Cd4 and recombinant Glycophorin B were included as negative control 'baits' and native Glycophorin A (MM) as a positive control

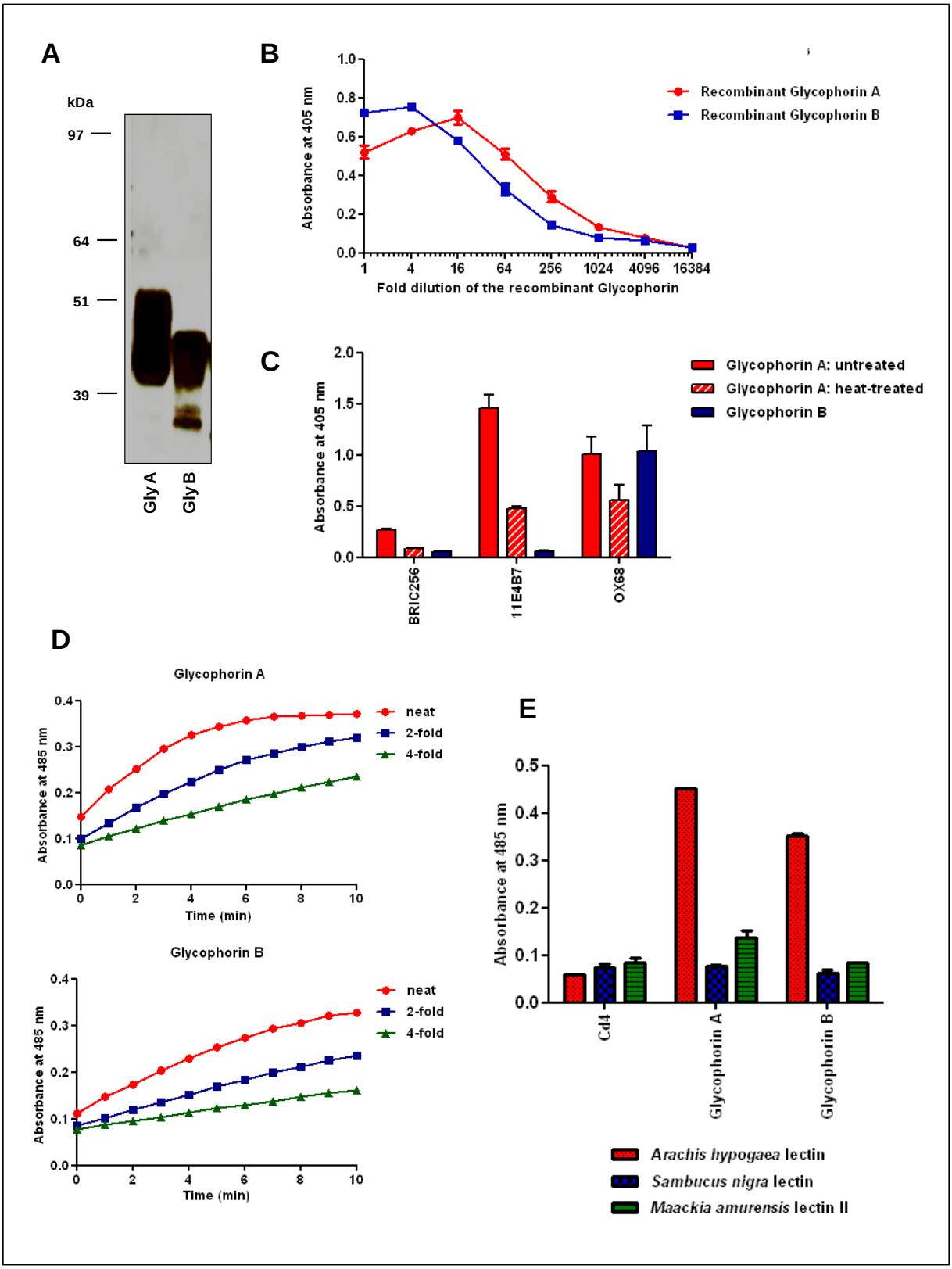
A
kDa
97
64
51
39
Gly A
Gly B
B
Absorbance at 405 nm
Fold dilution of the recombinant Glycophorin
Recombinant Glycophorin A
Recombinant Glycophorin B
C
Absorbance at 405 nm
Glycophorin A: untreated
Glycophorin A: heat-treated
Glycophorin B
BRIC256
11E4B7
OX68
D
Glycophorin A
Absorbance at 485 nm
Time (min)
neat
2-fold
4-fold
Glycophorin B
E
Absorbance at 485 nm
Cd4
Glycophorin A
Glycophorin B
Arachis hypogaea lectin
Sambucus nigra lectin
Maackia amurensis lectin II

Figure 15. The full-length ectodomain of human Glycophorin A was expressed in soluble form and characterised biochemically. Glycophorin A was expressed recombinantly using the HEK293E expression system, both as a monobiotinylated 'bait' and as a pentameric β-lactamase tagged 'prey'. The full-length ectodomain of Glycophorin B was similarly expressed for use as a control in downstream assays with Glycophorin A. **A)** Western blot of biotinylated Glycophorins A and B performed using HRP-conjugated extravidin as the probe. The expected molecular weight of an un-glycosylated monomer of Glycophorin A is 32.2 kDa. **B)** Quantitation of biotinylated Glycophorins A and B relative to each other by ELISA. The anti-Cd4 mouse monoclonal OX68, was used as the primary antibody. **C)** Recognition of untreated and heat-treated Glycophorin A by two mouse monoclonals, 11E4B7 and BRIC256, raised using human erythrocytes and native full-length Glycophorin A as immunogens respectively. Binding of these monoclonals was also detected by ELISA. Glycophorin B was used as a negative control 'bait' in the assays and OX68 as a positive control antibody. All ELISAs were performed on streptavidin-coated plates, using an alkaline phosphatase-conjugated anti-mouse antibody as the secondary. The data from ELISA assays are shown as mean ± standard deviation; *n*=3. **D)** Normalisation of pentameric β-lactamase tagged forms of Glycophorin A and B against each other by monitoring the turnover of nitrocefin at 485 nm over a period of 10 min. **E)** Analysis of the glycan composition of recombinant Glycophorin A, performed by testing its binding to three lectins. The biotinylated lectins were immobilised on a streptavidin coated-plate and incubated with β-lactamase tagged pentamers of Glycophorin A for 2 h at room temperature. Binding was subsequently detected by monitoring the turnover of nitrocefin at 485 nm. The glycan-binding specificities of the three lectins are as follows: *Arachis hypogaea* lectin (red)- non-sialylated Gal (β-1,3) GalNAc, *Sambucus nigra* lectin (blue)- terminal Neu5Ac (α-2,6) and *Maackia amurensis* lectin (green)- terminal Neu5Ac (α-2,3). Cd4 and Glycophorin B were used as controls in the assay. The bar chart shows mean ± standard deviation; *n*=3.

'bait' (Figure 16 A). Biotinylated OX68 was used as the positive control 'bait', when probing the 'prey' form of recombinant Glycophorin A against the *Pf*EBA175 FL 'bait' (Figure 16 B). Biotinylated Cd4 and pentameric Glycophorin B were used as the negative control 'bait' and 'prey' respectively in this experiment.

No interaction between recombinant human Glycophorin A and *Pf*EBA175 FL was observed in the AVEXIS assays.

3.2.6 No binding of recombinant Glycophorin A to *Pf*EBA175 FL was detected by SPR.

The ability of recombinant Glycophorin A to recognise *Pf*EBA175 FL was also tested using surface plasmon resonance, a method of very high sensitivity that allows protein-protein interactions to be monitored in real-time (van der Merwe, 2011).

To this purpose, the ectodomain of Glycophorin A was expressed with C-terminal Cd4 and hexa-His tags (Section 2.1.1 and Figure 4) and purified from the cell culture supernatant by affinity chromatography on a nickel-charged Sepharose column (Section 2.2.5) (Figure 17 A). The purified protein was analysed by SDS-PAGE under reducing conditions to confirm its expression at the correct size (Figure 17 B). The presence of carbohydrate moieties on recombinant Glycophorin A was verified by staining the polyacrylamide gel using a periodic acid-Schiff reagent method (Figure 17 C). The purified protein was then subjected to gel filtration to separate any aggregates that can confound SPR measurements and to exchange the protein into the SPR buffer. The protein eluted from the gel filtration column mainly as a monodisperse peak (Figure 17 D). The elution volume of the peak fraction, 34.9 ml, corresponds to an estimated size of approximately 60 kDa, suggesting that Glycophorin A was possibly eluting as a dimer.

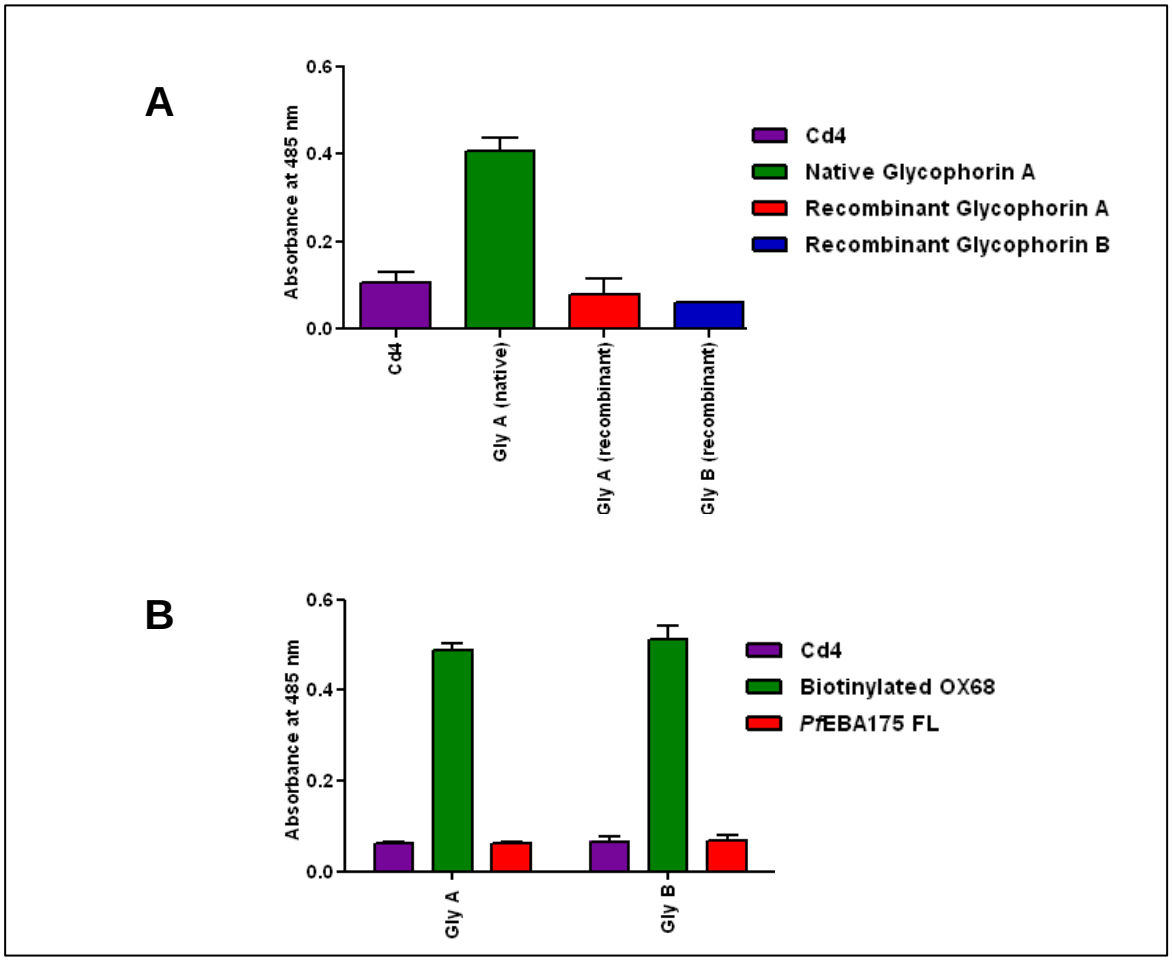

Figure 16. Recombinant human Glycophorin A was not recognized by *Pf*EBA175 FL. The AVEXIS assays were performed in two orientations. **A)** *Pf*EBA175 FL, in the pentameric, β-lactamase tagged 'prey' form, was tested against biotinylated recombinant Glycophorin A. Biotinylated native Glycophorin A was used as the positive control 'bait' in the assay and biotinylated Cd4 and Glycophorin B, the negative control 'baits'. **B)** Recombinant Glycophorin A, in the pentameric, β-lactamase tagged 'prey' form, was tested against biotinylated *Pf*EBA175 FL. Biotinylated OX68 and Cd4 were used as the positive and negative control 'baits' and recombinant Glycophorin B as the negative control 'prey'. The assays were performed on streptavidin-coated plates and the binding of the soluble 'preys' to the immobilised 'baits' was detected by monitoring the turnover of nitrocefin at 485 nm. The results are shown as mean ± standard deviation; *n*=3.

In the SPR experiment, the purified recombinant Glycophorin A was injected across biotinylated *Pf*EBA175 FL immobilised on a streptavidin-coated sensor chip. However, no interaction between the recombinant proteins could be detected (Figure 17 E). The activity of the immobilised *Pf*EBA175 FL was subsequently confirmed by injecting purified native Glycophorin A across the sensor surfaces (Figure 17 E).

3.2.7 The level of sialylation of recombinant Glycophorin A was increased by co-expression with sialyltransferases and a sialic acid transporter.

The inability of recombinant Glycophorin A to interact with *Pf*EBA175 FL could potentially be due to its lower levels of sialylation in comparison with native Glycophorin A (sections 3.2.3 and 3.2.4). Sialylation of recombinant proteins in mammalian systems has previously been shown to be increased by several strategies including supplementing the culture medium with sialic acid precursors (Gu & Wang, 1998) and co-expression of the glycoproteins-of-interest with Golgi-targeted sialyltransferases (Chitlaru *et al.*, 1998; Weikert *et al.*, 1999; Hossler et *al.*, 2009) or the CMP-sialic acid transporter (Wong *et al.*, 2006). Whereas sialyltransferases catalyse the addition of sialic acid moieties to the termini of N- and O-linked oligosaccharides, the CMP-sialic acid transporter mediates the trafficking of CMP-sialic acid from the cytosol into the Golgi lumen.

To try and increase its level of sialylation, recombinant Glycophorin A was co-expressed with the Golgi apparatus-targeted human α-2,3-sialyltransferase 1 (NP_003024.1), which catalyses the synthesis of the 'Neu5Ac (α-2,3) Gal' sequence on O-linked glycans, either singly or in combination with the rat α-2,6-sialyltransferase 1 (NP_001106815.1) or the human CMP-sialic acid transporter (NP_006407.1). The plasmids encoding the sialyltransferases and the CMP-sialic acid transporter were co-transfected with the Glycophorin A expression construct in either

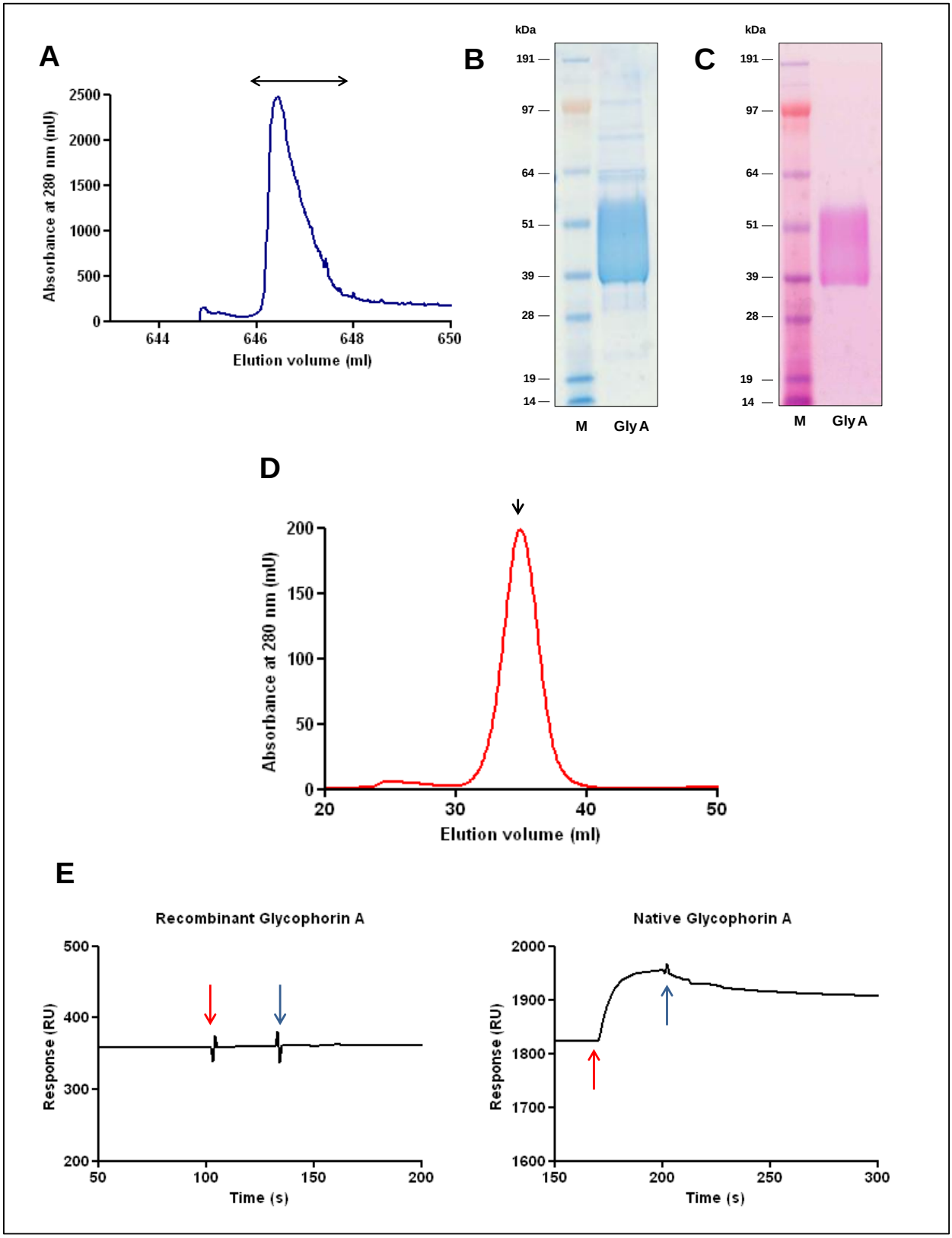
A
Absorbance at 280 nm (mU)
2500
2000
1500
1000
500
0
644
646
648
650
Elution volume (ml)
B
kDa
191
97
64
51
39
28
19
14
M
Gly A
C
kDa
191
97
64
51
39
28
19
14
M
Gly A
D
Absorbance at 280 nm (mU)
200
150
100
50
0
20
30
40
50
Elution volume (ml)
E
Recombinant Glycophorin A
Response (RU)
500
400
300
200
50
100
150
200
Time (s)
Native Glycophorin A
Response (RU)
2000
1900
1800
1700
1600
150
200
250
300
Time (s)

Figure 17. No interaction between recombinant human Glycophorin A and *Pf*EBA175 FL was detected by SPR. A) Hexa-His tagged Glycophorin A was purified from the culture supernatant by affinity chromatography on a nickel-charged sepharose column. The eluant from the column was monitored at 280 nm in real-time and the peak fractions containing protein (indicated by ⟷) were pooled. The affinity purified protein was analysed by SDS-PAGE and visualised using Coomassie brilliant blue **(B)** and a glycoprotein-specific staining method **(C)**. **D)** The elution profile of Glycophorin A from gel filtration. The peak fraction at ~35 ml is indicated by ↓. **E)** Reference subtracted sensorgrams from SPR analysis. Gel filtered-recombinant Glycophorin A (at 10 µM) and subsequently sialylated native Glycophorin A (at an approximately equivalent concentration) were injected at a flow rate of 30 µl/min, for 30 s across biotinylated *Pf*EBA175 and Cd4 (reference) immobilised on a streptavidin-coated sensor chip. The red and blue arrows indicate the start and the end of the 'prey' injections, respectively. The baits, *Pf*EBA175 FL and Cd4 (reference) were immobilised at molar equivalent amounts, *Pf*EBA175 FL- 2084 RU and Cd4- 261 RU respectively.

a 1:10 or a 1:5 ratio. The culture medium was additionally supplemented with the sialic acid precursor, N-acetyl-D-mannosamine, when the CMP-sialic acid transporter was co-transfected. The effects of these strategies on the glycan composition of recombinant Glycophorin A was analysed by testing β-lactamase tagged pentamers of Glycophorin A, expressed under the different conditions, against the lectins from *Arachis hypogaea*, *Sambucus nigra* and *Maackia amurensis* as described before (Section 3.2.4) (Figure 18). Co-transfection of Glycophorin A with the α-2,3-sialyltransferase 1 resulted in a clear increase in the level of glycans with terminal Neu5Ac (α-2,3), and this was further improved by co-transfection with the CMP-sialic acid transporter and supplementation with N-acetyl-D-mannosamine. Co-transfection with both α-2,3-sialyltransferase 1 and α-2,6-sialyltransferase 1, increased the level of terminal Neu5Ac (α-2,6) but had no noticeable effect on the Neu5Ac (α-2,3) level. Overall however the strategies were not effective enough to improve the sialylation of recombinant Glycophorin A to the levels observed in the native protein (Figure 18 B).

The sialylation-enhanced forms of recombinant Glycophorin A were tested against *Pf*EBA175 FL by AVEXIS and SPR as described previously. No binding of recombinant Glycophorin A to *Pf*EBA175 FL was observed (data not shown).

3.2.8 Kinetic parameters for the interaction between native Glycophorin A and *Pf*EBA175 FL were estimated by SPR.

Although recombinant Glycophorin A could not be produced in a form that bound to *Pf*EBA175, mechanistic insights can still be gleaned by investigating the binding of *Pf*EBA175 FL to native Glycophorin A, using SPR.

To perform this experiment, it was first necessary to identify a suitable method for immobilising the native Glycophorin A preparations (MM, MN and asialylated) on a SPR sensor chip. Direct

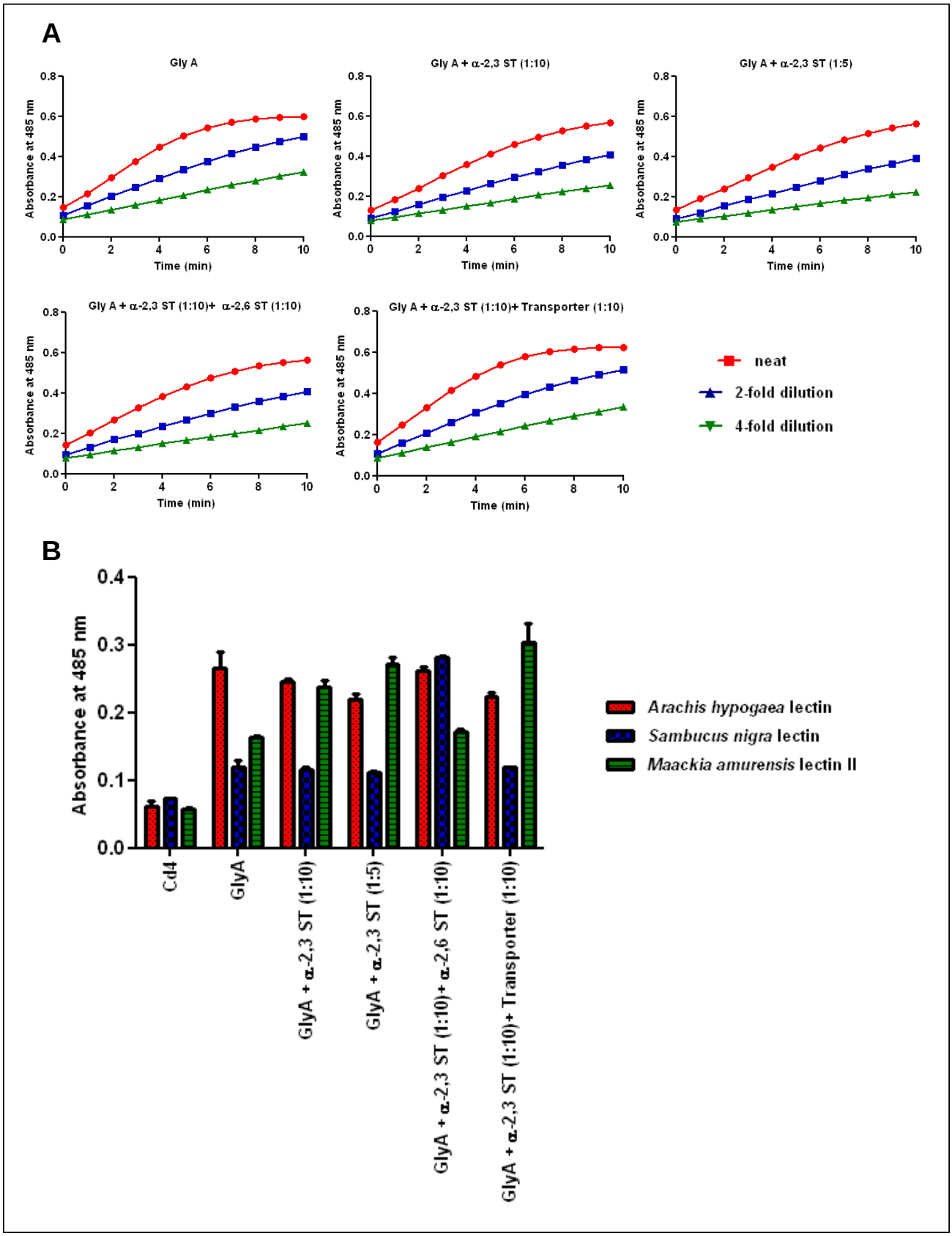
A
Gly A
Gly A + α-2,3 ST (1:10)
Gly A + α-2,3 ST (1:5)
Gly A + α-2,3 ST (1:10)+ α-2,6 ST (1:10)
Gly A + α-2,3 ST (1:10)+ Transporter (1:10)
Absorbance at 485 nm
Time (min)
neat
2-fold dilution
4-fold dilution
B
Absorbance at 485 nm
Cd4
GlyA
GlyA + α-2,3 ST (1:10)
GlyA + α-2,3 ST (1:5)
GlyA + α-2,3 ST (1:10)+ α-2,6 ST (1:10)
GlyA + α-2,3 ST (1:10)+ Transporter (1:10)
Arachis hypogaea lectin
Sambucus nigra lectin
Maackia amurensis lectin II

Figure 18. The sialylation of recombinant Glycophorin A was improved by co-expression with sialyltransferases and a sialic acid transporter. To potentially enhance its sialylation, recombinant Glycophorin A was co-expressed with the human α-2,3-sialyltransferase 1 (α-2,3 ST) either singly or in combination with the rat α-2,6-sialyltransferase 1 (α-2,6 ST) or the human CMP-sialic acid transporter. The expression plasmids encoding the transferases and the transporter were co-transfected with the Glycophorin A expression constructs either in a 1:5 or a 1:10 ratio. When the transporter was co-transfected, the culture medium was supplemented with 20 mM N-acetyl-D-mannosamine, a sialic-acid precursor. **A)** β-lactamase tagged pentamers of Glycophorin A expressed under the different conditions were normalised by monitoring the turnover of nitrocefin at 485 nm in a time-course assay. **B)** Analysis of the glycan composition of recombinant Glycophorin A pentamers, performed by testing their binding to three lectins. The biotinylated lectins were immobilised on a streptavidin coated-plate and incubated with β-lactamase tagged pentamers of Glycophorin A for 2 h at room temperature. Binding was subsequently detected by monitoring the turnover of nitrocefin at 485 nm. The glycan-binding specificities of the three lectins are as follows: *Arachis hypogaea* lectin (red)- non-sialylated Gal (β-1,3) GalNAc, *Sambucus nigra* lectin (blue)- terminal Neu5Ac (α-2,6) and *Maackia amurensis* lectin (green)- terminal Neu5Ac (α-2,3). Cd4 was used as a negative control in the assay. The bar chart shows mean ± standard deviation; *n*=3.

covalent attachment to a carboxymethylated dextran sensor surface via primary amine groups was tested as the first strategy. Covalent immobilisation is dependent on electrostatic pre-concentration of the ligand on the sensor surface, therefore to determine suitable coupling conditions, pre-concentration of Glycophorin A on the sensor chip surface was tested at a range of different pHs, by injecting the protein preparations across a non-activated sensor chip surface in short pulses, as recommended in the Biacore sensor surface handbook (*GE Healthcare*) (Figure 19 A). Electrostatic pre-concentration is dependent on the sensor surface and the injected ligand carrying opposite net charges, therefore the range of pHs tested was based on the predicted isoelectric point of unglycosyalted Glycophorin A (5.15) and the pK_a of the sensor chip surface (3.5). Whereas asialylated Glycophorin A showed increasingly efficient pre-concentration (observed as an increase in the response) at pHs 5.5 to 4.5, no electrostatic binding of Glycophorin A (MN) could be observed even at pH 4.0, suggesting that sialylated Glycophorin A might be too acidic to bind efficiently to carboxymethylated dextran. Both Glycophorin A (MN) and asialylated Glycophorin A were subsequently injected across a NHS/EDC-activated carboxymethyl dextran sensor surface, at a pH of 4.5, to check for covalent immobilisation (Figure 19 B). As expected, only asialylated Glycophorin A showed binding to the sensor surface. It was therefore necessary to find an alternative immobilisation strategy for Glycophorin A that was not dependent on electrostatic pre-concentration. To this purpose, native Glycophorin A preparations were tested for binding to a streptavidin-coated sensor chip, after biotinylation *in vitro*. This approach was observed to be suitable for immobilising both sialylated and asialylated forms of Glycophorin A (Figure 19 C).

For testing against native Glycophorin A by SPR, *Pf*EBA175 FL was expressed with C-terminal Cd4 and hexa-His tags and purified from harvested culture supernatant by affinity

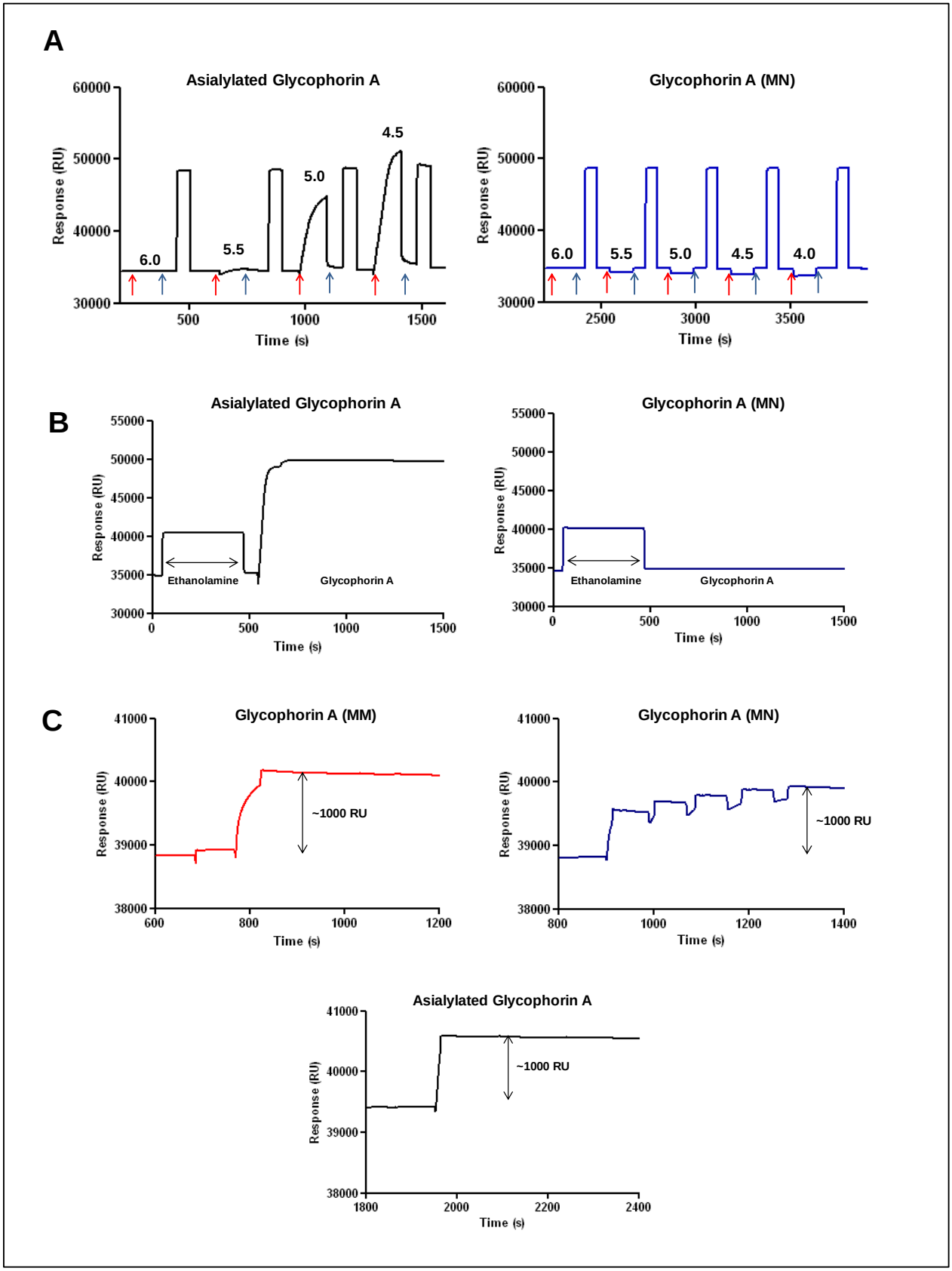
A
Asialylated Glycophorin A
Response (RU)
Time (s)
6.0
5.5
5.0
4.5
Glycophorin A (MN)
6.0
5.5
5.0
4.5
4.0
B
Asialylated Glycophorin A
Ethanolamine
Glycophorin A
Glycophorin A (MN)
Ethanolamine
Glycophorin A
C
Glycophorin A (MM)
~1000 RU
Glycophorin A (MN)
~1000 RU
Asialylated Glycophorin A
~1000 RU

Figure 19. Immobilisation of native Glycophorin A on SPR sensor chips. The native Glycophorin A preparations were tested for immobilisation on both carboxymethylated dextran-coated (CM5) and streptavidin-coated sensor chips. **A)** Testing the Glycophorin A preparations for electrostatic pre-concentration on a non-activated CM5 sensor chip, at different pHs. The protein preparations were injected at 50 µg/ml in 10 mM sodium acetate buffer of varying pH, using a flow rate of 10 µl/min for 120 s. The red and blue arrows indicate the start and the end respectively of these 'bait' injections. Each injection of Glycophorin A was followed by a 60 s injection of 1 M ethanolamine-HCl (pH 8.5) to remove any electrostatically-bound protein. **B)** Testing the Glycophorin A preparations for covalent immobilisation on the CM5 sensor chip at a pH of 4.5. Prior to injecting the protein the sensor surface was activated with a pulse of 0.2 M EDC and 0.05 M NHS. **C)** Immobilisation of the Glycophorin A preparations on a streptavidin-coated sensor chip after *in vitro* biotinylation. The proteins were injected in HBS buffer at a flow rate of 10 µl/min.

chromatography on nickel-charged Sepharose (Figure 20 A). Analysis of the purified protein by SDS-PAGE under reducing conditions, confirmed its expression at the expected size of 184.2 kDa (Figure 20 B). Some of the protein however appeared to be N-terminally processed, generating shorter fragments. Separation of the full-length form of the protein from the processed fragments was attempted with gel filtration (Figure 20 C). The expected elution volumes of monomeric (184.2 kDa) and dimeric (368.4 kDa) forms of *Pf*EBA175 FL were 29.38 and 26.42 ml respectively. The observed elution profile of *Pf*EBA175 FL consisted of four peaks at 25.14, 28.65, 33.46 and 39.08 ml. The elution volumes suggest that peaks 1 and 2 contained dimers and monomers of *Pf*EBA175 FL respectively, whereas peaks 3 and 4 carried shorter processed fragments. This was confirmed to some extent by analysing the peak fractions using denaturing SDS-PAGE and silver staining (Figure 20 D). Peaks 1 and 2 were observed to be enriched in the full-length form of the protein, whereas peaks 3 and 4 predominantly contained processed fragments at ~60 kDa and ~40 kDa respectively. Although 1 µg of protein from each of peaks 1 and 2 were loaded onto the gel, only some of the protein from peak 1 appeared to have entered the gel. This could be due to some dimers (or higher-order aggregates) persisting after heat-denaturation and not passing through the polyacrylamide matrix.

When the four peak fractions of *Pf*EBA175 FL were injected across native Glycophorin A immobilised on the streptavidin-coated SPR sensor chip, the highest binding to both MM and MN types of sialylated Glycophorin A was observed with peak fraction 2, containing monomeric *Pf*EBA175 FL (Figure 21 A). No binding of the peak fractions to asialylated Glycophorin A was observed.

To derive equilibrium and kinetic parameters for its interaction with native Glycophorin A, a 2-fold dilution series of monomeric *Pf*EBA175 FL was injected across the SPR sensor chip

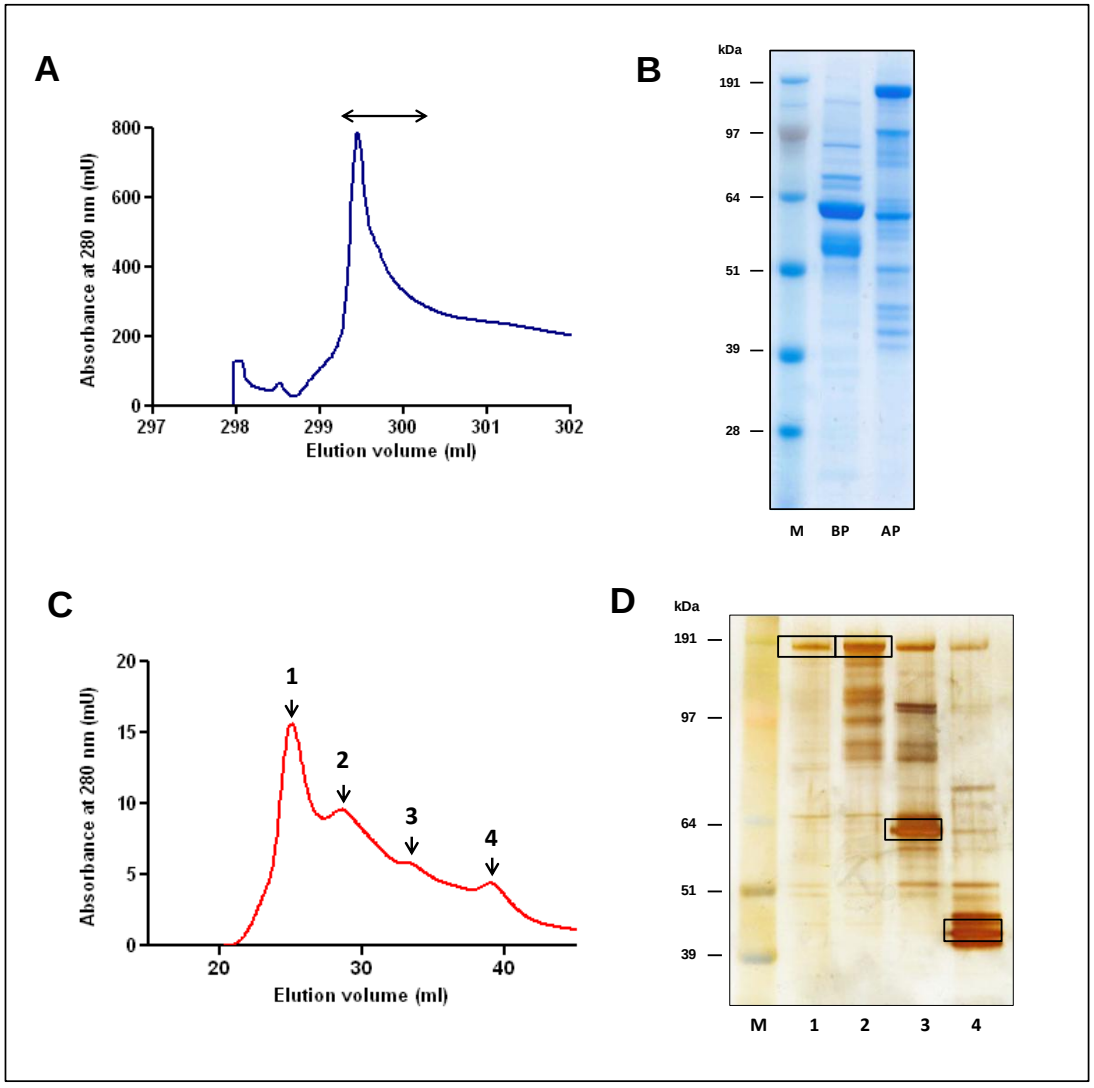

Figure 20. *Pf*EBA175 FL was expressed in soluble, hexa-His tagged form and purified from the culture supernatant. A) *Pf*EAB175 FL was purified from the culture supernatant by affinity chromatography on a nickel-charged Sepharose column. The eluant from the column was monitored at 280 nm in real-time and the peak fractions containing protein (indicated by ↓) were pooled. **B)** The affinity purified protein was analysed by SDS-PAGE and visualised using Coomassie brilliant blue. BP- before purification, AP- after purification. **C)** The elution profile of *Pf*EBA175 FL from gel filtration. The four peak fractions at 25.14 (1), 28.65 (2), 33.46 (3) and 39.08 ml (4) are indicated by ↔ . **D)** The peak fractions of *Pf*EBA175 FL from gel filtration were analysed by SDS-PAGE and visualised by silver staining. 1 µg of peak fractions 1 and 2 were loaded onto the gel and 0.5 µg of fractions 3 and 4. The most prominent band on each lane of the gel is boxed-in.

surfaces as described in Section 2.5.3 (Figure 21 B). Each set of binding curves (sensorgrams) obtained after reference subtraction (i.e. binding to Glycophorin A- binding to Cd4 immobilised in flow cell 1) was first evaluated for affinity, by plotting response at equilibrium (when association= dissociation, so that there is no net binding) against *Pf*EBA175 FL concentration (Figure 22 A). The data sets were fitted globally to a steady-state 1:1 binding model to derive the equilibrium dissociation constant, K_D. The Chi^2 (R^2) value, a measure of the difference between the experimental data and the fitted curve, was taken into account as an indication of the fidelity of the fit. The K_D values computed for MM and MN types of Glycophorin A were (2.8 ± 0.7) x 10^{-7} M and (2.1 ± 0.5) x 10^{-7} M respectively. The fitting of the model to the data sets were acceptable with corresponding R^2 values of 5.70 and 14.6. The difference in K_D values suggests that *Pf*EBA175 FL was binding to MN Glycophorin with a slightly higher affinity than to MM Glycophorin.

For kinetic evaluation, the data sets were globally fitted to a simple 1:1 binding model and to a more complicated two state reaction model (Figure 22 B). The latter assumes a 1:1 binding of the analyte to the immobilised ligand followed by a conformational change that stabilises the complex and was selected based on the 'ligand-induced dimerisation model' for the EBA175-Glycophorin A interaction proposed by Tolia *et al*. (2005). The two sets of binding curves obtained from the interaction of *Pf*EBA175 FL with MM and MN Glycophorin A were observed to show a much better fit (lower R^2) to the two state reaction model than to the 1:1 binding model (Figure 22 C). The K_D values calculated from the k_d/k_a parameters deduced using the two state reaction model, were also closer to the K_D values estimated from the equilibrium analysis.

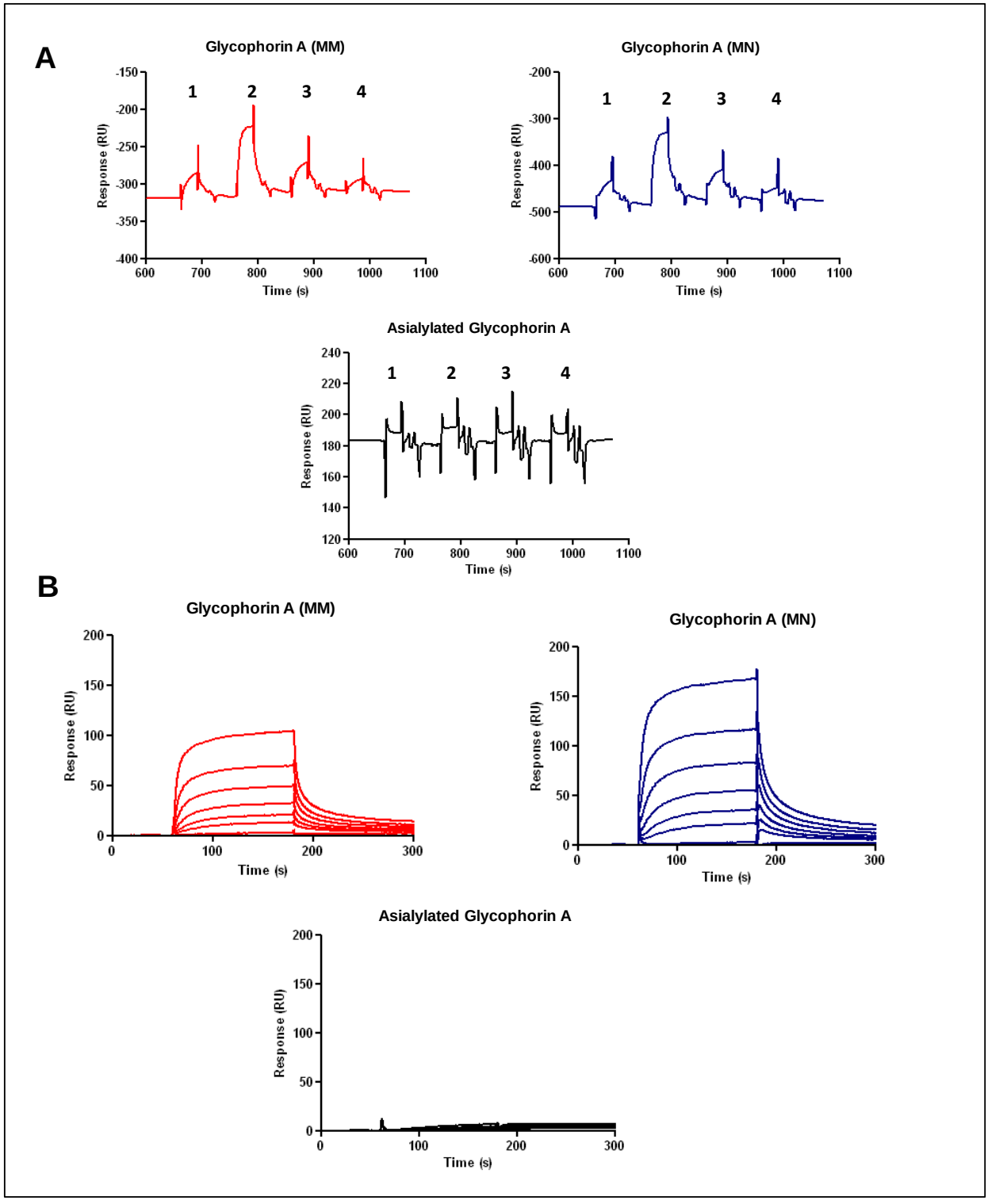
A
Glycophorin A (MM)
Response (RU)
Time (s)
1
2
3
4
Glycophorin A (MN)
Response (RU)
Time (s)
1
2
3
4
Asialylated Glycophorin A
Response (RU)
Time (s)
1
2
3
4
B
Glycophorin A (MM)
Response (RU)
Time (s)
Glycophorin A (MN)
Response (RU)
Time (s)
Asialylated Glycophorin A
Response (RU)
Time (s)

Figure 21. The binding of *Pf*EBA175 FL to native Glycophorin A was analysed by SPR. Reference subtracted sensorgrams from the injection of the four peak fractions of *Pf*EBA175 FL from gel filtration **(A)** or a 2-fold dilution series of peak fraction 2 **(B)**, across biotinylated native Glycophorin A immobilised on a streptavidin-coated sensor chip. The binding to Glycophorin A (MM), Glycophorin A (MN) and asialylated Glycophorin A are shown in red, blue and black respectively. The biotinylated baits were immobilised at Cd4 (reference)-1000 RU , Glycophorin A (MM)-1267 RU, Glycophorin A (MN)-1070 RU and asialylated Glycophorin A-1170 RU. **A)** The peak fractions with estimated concentrations of 380 nM (peak 1), 300 nM (peak 2), 180 nM (peak 3) and 150 nM (peak 4) were injected across the sensor chip surfaces at a flow rate of 30 µl/min, for 60 s each. **B)** The concentration series of *Pf*EBA175 FL, ranging from 93-300 nM, was injected at a flow rate of 20 µl/min, with a contact time of 120 s and a dissociation time of 200 s. At the end of each injection the sensor surface was regenerated with a pulse of 5 M NaCl.

A

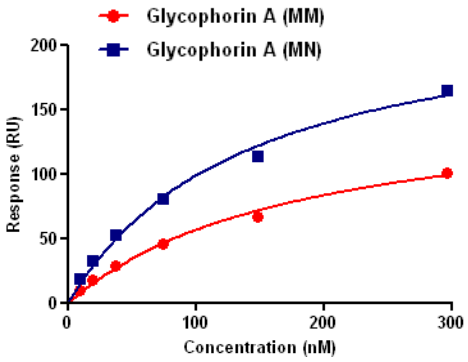

B

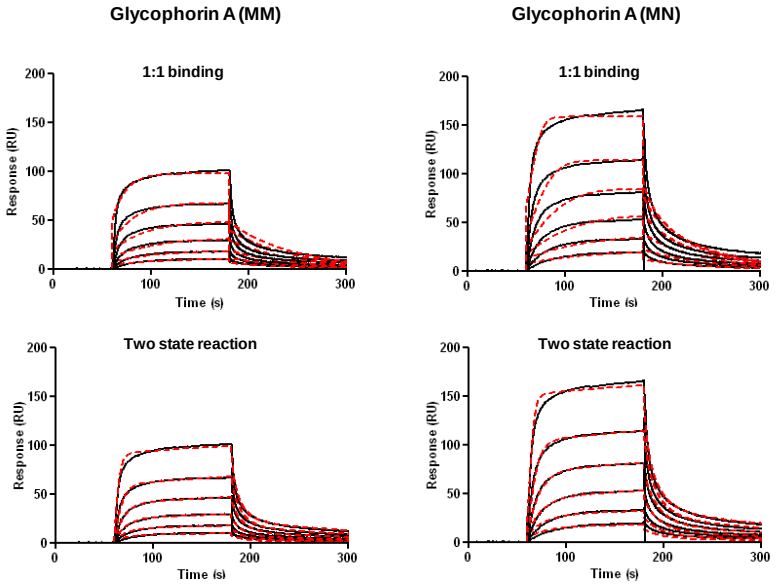

C

Glycophorin A (MM)				
Model	**Chi² (R^2)**	**k_a ($M^{-1}s^{-1}$)**	**k_d (s^{-1})**	**K_D (M)**
Steady-state affinity	5.70			$(2.8 \pm 0.7) \times 10^{-7}$
1:1 binding (kinetic)	12.9	$(2.10 \pm 0.04) \times 10^{5}$	$(1.57 \pm 0.03) \times 10^{-2}$	0.75×10^{-7}
Two state reaction (kinetic)	1.72	I $(1.40 \pm 0.02) \times 10^{9}$ II $(5.1 \pm 0.1) \times 10^{-3}$	I 302.0 ± 3.7 II $(2.83 \pm 0.06) \times 10^{-3}$	1.38×10^{-7}

Glycophorin A (MN)				
Model	**Chi² (R^2)**	**k_a ($M^{-1}s^{-1}$)**	**k_d (s^{-1})**	**K_D (M)**
Steady-state affinity	14.6			$(2.1 \pm 0.5) \times 10^{-7}$
1:1 binding (kinetic)	24.4	$(2.5 \pm 0.2) \times 10^{6}$	0.17 ± 0.01	0.70×10^{-7}
Two state reaction (kinetic)	4.36	I $(1.14 \pm 0.01) \times 10^{9}$ II $(2.58 \pm 0.06) \times 10^{-3}$	I 178.7 ± 1.2 II $(5.0 \pm 0.2) \times 10^{-3}$	1.03×10^{-7}

Figure 22. Equilibrium and kinetic parameters for the interaction of *Pf*EBA175 FL with native Glycophorin A were derived from the SPR data. The reference subtracted SPR sensorgrams from the binding of *Pf*EBA175 FL to MM and MN types of native Glycophorin A were subjected to equilibrium **(A)** and kinetic **(B)** analysis. **A)** For each set of sensorgrams the response at equilibrium was plotted as a function of *Pf*EBA175 FL concentration and globally fitted to a steady-state 1:1 binding model to obtain an estimate of the K_D. **B)** To obtain estimates of kinetic parameters, the sensorgrams were globally fitted to two models, simple 1:1 binding and a more complex two-state reaction. The black lines represent experimental data and the red dotted lines, the fitted curves. **C)** Tables with equilibrium and kinetic parameters estimated for the *Pf*EBA175 FL- Glycophorin A interaction using the different models. For each model, the fit to the experimental data is indicated as the Chi^2 value (i.e. average squared residuals). The estimated values for the k_a, k_d and K_D are indicated with the standard error.

3.2.9 *Pf*EBA175 RII was produced in soluble form and its interaction with native Glycophorin A was probed.

The vast majority of the previous studies on the *Pf*EBA175-Glycophorin A interaction have been carried out using *Pf*EBA175 RII. In order to determine whether *Pf*EBA175 RII binds to native Glycophorin A with the same affinity as *Pf*EBA175 FL, the SPR experiment described in the previous section was repeated with *Pf*EBA175 RII.

In order to express *Pf*EBA175 RII, the segment of the coding sequence for this region of the extracellular domain was PCR-amplified from an expression construct of *Pf*EBA175 FL (Figure 23 A), digested with the restriction endonucleases NotI and AscI and then cloned into a NotI/AscI- digested expression vector that would enable it to be expressed with C-terminal Cd4 and hexa-His tags, as described in Section 2.1.1 (Figure 23 B).

After expression, *Pf*EBA175 RII was purified from the culture supernatant as described before for *Pf*EBA175 FL (Figure 23 C), analysed by SDS-PAGE (Figure 23 D) and subjected to gel filtration immediately prior to SPR (Figure 23 E). The expected elution volume of a monomer of *Pf*EBA175 RII (97.52 kDa) from the gel filtration column was 32 ml. The observed elution profile of the protein consisted of a single peak with the highest absorbance at 34.6 ml. A sample of the protein was subsequently sent for analysis by size exclusion chromatography-multi angle light scattering (SEC-MALS) and found to be present predominantly in the monomeric form with a small degree of self-association (data not shown, the analysis was performed by Dr. Steven Johnson, University of Oxford).

In the SPR experiment, a 2-fold dilution series of gel filtered-*Pf*EBA175 RII was injected across native Glycophorin A preparations (MM, MN and asialylated) immobilised on a streptavidin-coated sensor chip (Figure 23 F). The sets of binding curves obtained after reference subtraction

were first fitted globally to a steady-state 1:1 binding model to estimate the K_D, as described previously for *Pf*EBA175 FL (Figure 24 A). The values obtained for MM and MN types of Glycophorin A, (26.1 ± 1.6) x 10^{-7} M and (20.2 ± 1.6) x 10^{-7} M respectively, suggest not only that *Pf*EBA175 RII was binding to MN Glycophorin A with a higher affinity than to MM Glycophorin A, but also that the interaction of native Glycophorin A with *Pf*EBA175 RII is about 10-fold weaker than its binding to *Pf*EBA175 FL. As before the data sets were also fitted to two kinetic models, 1:1 binding and two-state reaction (Figure 24 B). The experimental data sets fitted more closely to the two-state reaction model than to the 1:1 binding model and the K_D values calculated from the k_a/k_d parameters deduced using the two state reaction model, were also closer to the K_D values estimated from the steady-state affinity analysis (Figure 24 C).

3.3 DISCUSSION

Since its first identification almost three decades ago (Camus and Hadley, 1985), the *P. falciparum* antigen, *Pf*EBA175 FL, has remained a subject of rigorous scientific investigation. Although not essential for the invasion of erythrocytes by *P. falciparum*, *Pf*EBA175 is postulated to play an important functional role in both sialic acid-dependent and -independent strains of *P. falciparum* (Duraisingh *et al*., 2003). Antibodies raised against *Pf*EBA175 inhibit erythrocyte entry by both types of strains (Narum *et al*., 2000) and deletion of *Pf*EBA175 leads to a change in the expression of other invasion ligands in sialic acid-dependent strains like W2mef as well as in those such as 3D7 which do not require sialic acid for invasion (Duraisingh *et al*., 2003; Lopaticki *et al*., 2011). The sialic acid-dependent interaction of native *Pf*EBA175 with Glycophorin A on the erythrocyte surface was identified from studies using enzymatically pre-treated erythrocytes as well as polymorphic erythrocytes lacking sialic acid on O-linked

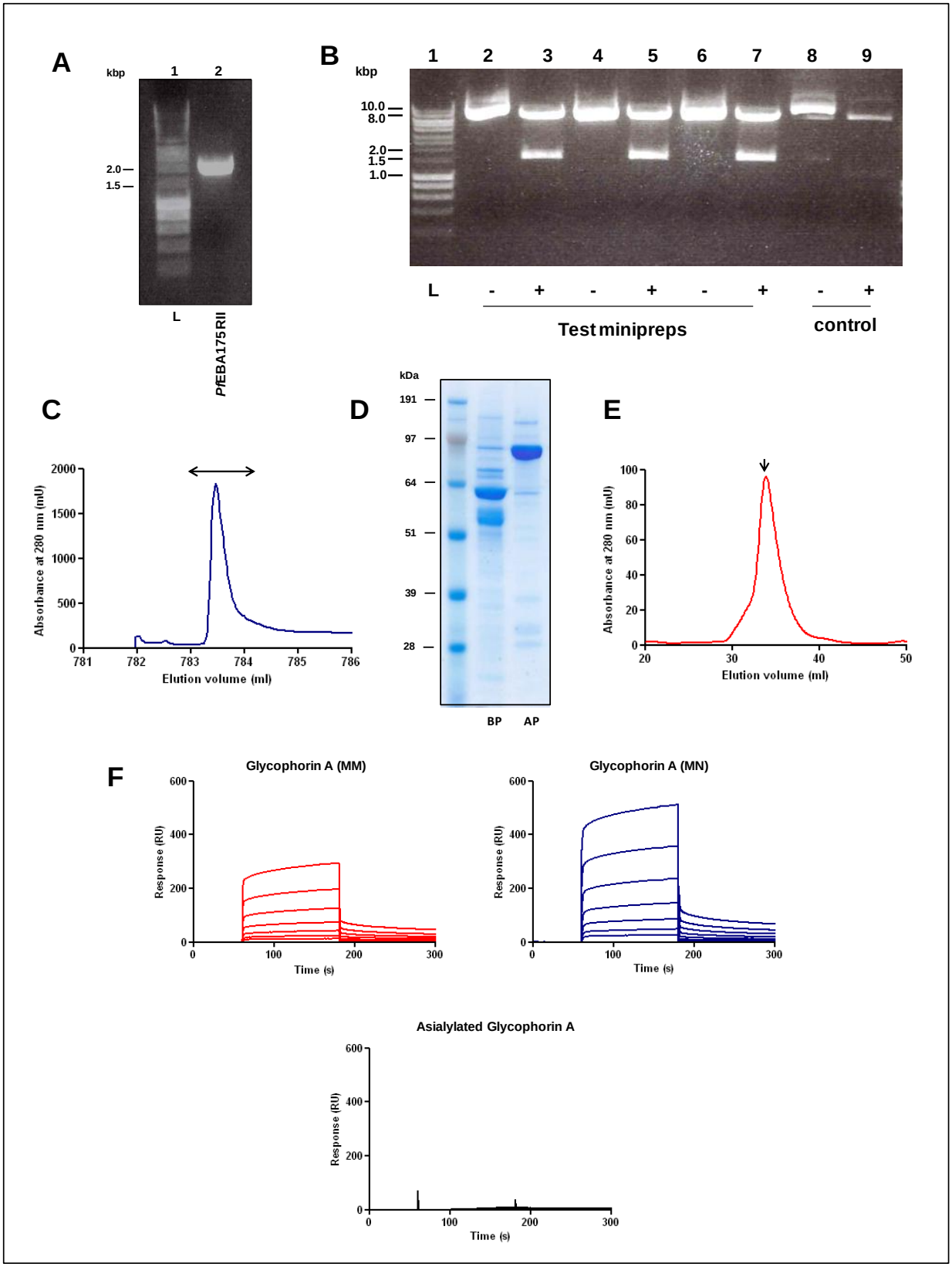
A
kbp
1
2
2.0
1.5
L
PfEBA175RII
B
kbp
1 2 3 4 5 6 7 8 9
10.0
8.0
2.0
1.5
1.0
L
- + - + - + - +
Test minipreps
control
C
Absorbance at 280 nm (mU)
2000
1500
1000
500
0
781 782 783 784 785 786
Elution volume (ml)
D
kDa
191
97
64
51
39
28
BP
AP
E
Absorbance at 280 nm (mU)
100
80
60
40
20
0
20 30 40 50
Elution volume (ml)
F
Glycophorin A (MM)
Response (RU)
600
400
200
0
0 100 200 300
Time (s)
Glycophorin A (MN)
Response (RU)
600
400
200
0
0 100 200 300
Time (s)
Asialylated Glycophorin A
Response (RU)
600
400
200
0
0 100 200 300
Time (s)

0

Figure 23. *Pf*EBA175 RII was expressed in soluble form and its binding to native human Glycophorin A was analysed by SPR. A) The region of the coding sequence for *Pf*EBA175 RII was amplified from an expression plasmid of *Pf*EBA175 FL by PCR. The expected length of the PCR product was 1.9 kbp. The PCR-amplified sequence was ligated into a vector (for expression with C-terminal Cd4 and hexa-His tags) using NotI and AscI restriction sites. **B)** After propagation in *E. coli*, the purified recombinant plasmids were tested for the presence of an insert of the expected size by digestion with NotI and AscI (+). Control reactions were set up with no enzymes (-). **C)** His-tagged *Pf*EAB175 RII was purified from the culture supernatant by affinity chromatography on a nickel-charged Sepharose column. The eluant from the column was monitored at 280 nm in real-time and the peak fractions containing protein (indicated by ⟷) were pooled. **D)** The affinity purified protein was analysed by SDS-PAGE and visualised using Coomassie brilliant blue. BP- before purification, AP- after purification. **E)** The elution profile of *Pf*EBA175 FL from gel filtration. The peak fraction at 34.6 ml is indicated by ↓. **F)** Reference subtracted sensorgrams from the injection of a 2-fold dilution series, ranging from 2.9-0.045 µM, of the main peak fraction of gel filtered-*Pf*EBA175 RII across biotinylated native Glycophorin A immobilised on a streptavidin-coated sensor chip. The binding to Glycophorin A (MM), Glycophorin A (MN) and asialylated Glycophorin A are shown in red, blue and black respectively. The biotinylated baits were immobilised at Cd4 (reference)-1000 RU , Glycophorin A (MM)-1267 RU, Glycophorin A (MN)-1070 RU and asialylated Glycophorin A-1170 RU. *Pf*EBA175 RII was injected at a flow rate of 20 µl/min, with a contact time of 120 s and a dissociation time of 200 s. At the end of each injection the sensor surface was regenerated with a pulse of 5 M NaCl.

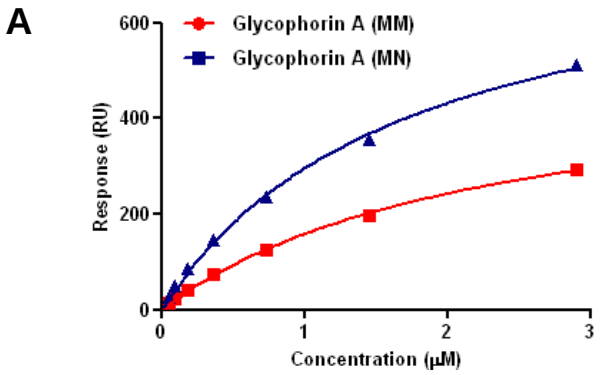

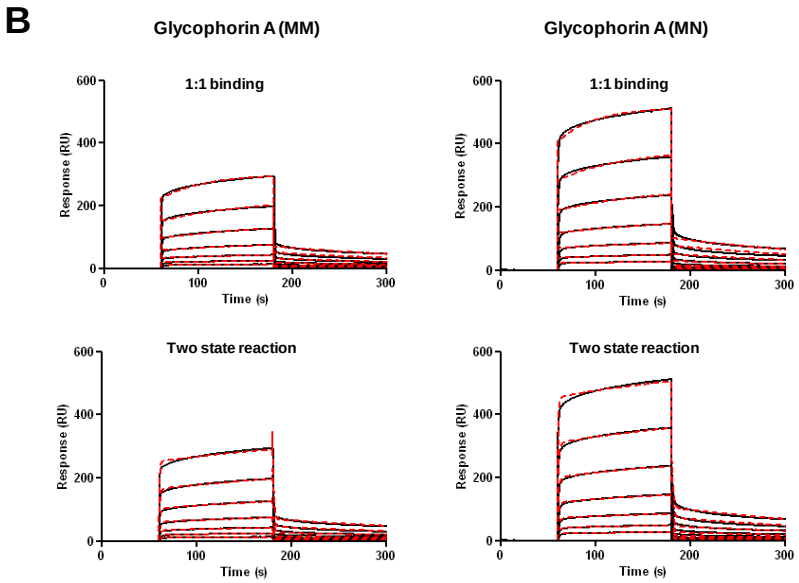

C

Glycophorin A (MM)				
Model	**Chi² (R^2)**	**k_a ($M^{-1}s^{-1}$)**	**k_d (s^{-1})**	**K_D (M)**
Steady-state affinity	5.9			$(26.1 \pm 1.6) \times 10^{-7}$
1:1 binding (kinetic)	25.2	6251 ± 170	$(3.58 \pm 0.09) \times 10^{-3}$	5.79×10^{-7}
Two state reaction (kinetic)	6.8	I $(7.7 \pm 0.6) \times 10^{5}$ II $(2.208 \pm 0.008) \times 10^{-3}$	I 2.7 ± 0.2 II $(3.10 \pm 0.02) \times 10^{-3}$	21.34×10^{-7}

Glycophorin A (MN)				
Model	**Chi² (R^2)**	**k_a ($M^{-1}s^{-1}$)**	**k_d (s^{-1})**	**K_D (M)**
Steady-state affinity	28.3			$(20.2 \pm 1.6) \times 10^{-7}$
1:1 binding (kinetic)	40.3	6203 ± 160	$(3.53 \pm 0.09) \times 10^{-3}$	5.49×10^{-7}
Two state reaction (kinetic)	17.5	I $(2.52 \pm 0.02)\ 10^{5}$ II $(2.216 \pm 0.009) \times 10^{-3}$	I 0.884 ± 0.005 II $(3.09 \pm 0.02) \times 10^{-3}$	10.81×10^{-7}

Figure 24. Equilibrium and kinetic parameters for the interaction of *Pf*EBA175 RII with native Glycophorin A were derived from the SPR data. The reference subtracted SPR sensorgrams from the binding of *Pf*EBA175 RII to MM and MN types of native Glycophorin A were subjected to equilibrium **(A)** and kinetic **(B)** analysis. **A)** For each set of sensorgrams the response at equilibrium was plotted as a function of *Pf*EBA175 RII concentration and globally fitted to a steady-state 1:1 binding model to obtain an estimate of the K_D. **B)** To obtain estimates of kinetic parameters, the sensorgrams were globally fitted to two models, simple 1:1 binding and a more complex two-state reaction. The black lines represent experimental data and the red dotted lines, the fitted curves. **C)** Tables with equilibrium and kinetic parameters estimated for the *Pf*EBA175 RII-Glycophorin A interaction using the different models. For each model, the fit to the experimental data is indicated as the Chi^2 value (i.e. average squared residuals). The estimated values for the k_a, k_d and K_D are indicated with the standard errors.

tetrasaccharides (T_n) or deficient in Glycophorin A expression (Ena^- , M^kM^k) (Camus and Hadley, 1985; Orlandi *et al*., 1992). Primarily due to the inability to express the large (175 kDa) full-length ectodomain of *Pf*EBA175 in soluble recombinant form using traditional methods, much of the detailed biochemical characterisation of the *Pf*EBA175-Glycophorin A interaction, has been performed using a truncated fragment of the *Pf*EBA175 extracellular domain, RII, which contains the tandem DBL domains essential for erythrocyte binding (Sim *et al*., 1994). The possible involvement of the extracellular regions of *Pf*EBA175 outside of RII in Glycophorin A binding and/or erythrocyte invasion has therefore not been investigated. To enable such a role/s to be identified, the expression of the full-length ectodomain of *Pf*EBA175 (*Pf*EBA175 FL) in a biochemically-amenable manner, is a pre-requisite. In this study, a soluble recombinant *Pf*EBA175 FL antigen, produced in mammalian HEK293E cells, was extensively characterised using biochemical methods, both to confirm its similarity to native *Pf*EBA175 in terms of function and to gain mechanistic insight into its interaction with Glycophorin A.

3.3.1 Recombinant *Pf*EBA175 FL is functionally similar to native *Pf*EBA175 isolated from parasite cultures.

The production of *Pf*EBA175 FL in recombinant form was facilitated by codon-optimisation of its coding sequence, for mammalian expression, by gene synthesis. *P. falciparum* proteins are not glycosylated in the parasite (Gowda & Davidson, 1999), therefore structural similarity of the recombinant protein to native *Pf*EBA175 was ensured by removal of the potential N-linked glycosylation sites during gene assembly. Secretion of the protein into the culture medium after transient expression was achieved by replacement of the endogenous signal peptide with a mammalian leader sequence. The recombinant *Pf*EBA175 FL protein was observed to be expressed in the full-length form (Figure 9 A). It was also recognised by three anti-*Pf*EBA175

monoclonals, two of which are known to bind heat-labile epitopes, suggesting that it was correctly-folded, at least in RII (Figures 9 C and D).

The binding of recombinant *Pf*EBA175 FL to human erythrocytes was then investigated using a quantitative, flow cytometry-based assay. Multimeric arrays of *Pf*EBA175 FL, generated by immobilisation on fluorescent beads, showed trypsin and neuraminidase-sensitive, but chymotrypsin-resistant association with human erythrocytes (Figures 10 and 11), suggesting a specific sialic-acid dependent interaction with Glycophorin A (a trypsin-sensitive but chymotrypsin-resistant erythrocyte receptor). In addition to the enzymatic pre-treatments of cells, the Glycophorin A-dependency of the interaction was further confirmed by pre-incubation of erythrocytes with an anti-Glycophorin A monoclonal (BRIC256), which significantly decreased the binding of *Pf*EBA175 FL (Figure 12). These results suggest that the recombinant *Pf*EBA175 FL is functionally similar to native *Pf*EBA175.

The binding of *Pf*EBA175 FL to commercially-available native Glycophorin A was then tested in an ELISA-based assay, to validate the biochemical activity of the recombinant protein independently. *Pf*EBA175 FL was observed to recognise native Glycophorin A but not an asialylated derivative, indicating specificity (Figure 14). The Glycophorin preparations used in this assay, were pre-characterised both for the presence of Glycophorin A (by staining with the anti-Glycophorin A monoclonal, BRIC256) and for the presence/absence of covalently-linked sialic acid (by testing the binding to three lectins of known glycan-binding specificity) (Figure 13). Glycans with terminal α-2,3 linked sialic acid (Neu5Ac) were predominant in the native Glycophorin A preparations, whereas the asialyalted protein mainly contained the T antigen, Gal (β-1,3) GalNAc (Figure 13 A).

3.3.2 The kinetic profile of the binding of *Pf*EBA175 FL to native Glycophorin A is consistent with the 'ligand-induced dimerisation model'.

The binding of *Pf*EBA175 FL to native Glycophorin A was then probed by SPR to gain insight into the mechanistic basis of the interaction. For this purpose, *Pf*EBA175 FL was expressed with a C-terminal hexa-His tag and purified from the cell culture supernatant by affinity chromatography. Analysis of the purified protein by denaturing SDS-PAGE confirmed the presence of the full-length form, but also revealed the presence of a number of shorter fragments (Figure 20 B). These fragments were present at a lower abundance than the full-length form and are likely to be products of proteolytic processing, as the cell culture medium was not supplemented with protease inhibitors during protein expression. Such additional fragments can also be seen on immunoblots of *P. falciparum* culture supernatants, performed using anti-*Pf*EBA175 monoclonals as probes, suggesting that some processing of the native *Pf*EBA175 also occurs, after release from the parasite surface (Orlandi *et al*., 1990).

Analysis of purified recombinant *Pf*EBA175 FL by gel filtration revealed the presence of both (potential) dimers/oligomers and monomers of the full-length protein (Figures 20 C and D). The monomeric fraction of *Pf*EBA175 FL showed higher binding to native Glycophorin A than the dimeric/oligomeric fraction when probed by SPR, and was thus used for the subsequent kinetic analysis (Figure 21). The reference subtracted SPR sensorgrams obtained from the binding of *Pf*EBA175 FL to native Glycophorin A were clearly biphasic, with both the association and dissociation of the soluble analyte consisting of a 'fast' stage followed by a 'slow' stage. Such behaviour is characteristic of an in interaction involving a conformational change in the binding partners and indeed the sensorgrams globally fitted to a 'two-state reaction' kinetic model far better than to a simple '1:1 binding' kinetic model (Figure 22 B and C). The K_D values calculated

from the 'two-state reaction' model were also in closer agreement with the K_D values estimated from the equilibrium analysis (Figure 22 C). This binding data is therefore, consistent with the proposed 'ligand-induced dimerisation' model for the binding of *Pf*EBA175 to Glycophorin A, which postulates that monomeric *Pf*EBA175 assembles into a dimer around the dimeric Glycophorin A receptor (Tolia *et al*., 2005, Section 3.1.2).

The 'biphasic' characteristic of the SPR sensorgrams could however also be a consequence of the presence of protein aggregates in the soluble analyte sample. Due care was taken to separate out the potentially monomeric fraction of full-length *Pf*EBA175 FL from the rest, prior to SPR. However, as gel filtration, the technique used for this purpose, has relatively low resolution, the presence of contaminant aggregates in the monomer fraction cannot be ruled out.

3.3.3 The affinity of *Pf*EBA175 FL for MN Glycophorin A is x 1.3-fold higher than that for MM Glycophorin A.

The binding of *Pf*EBA175 FL to native Glycophorin A isolated from both MM and MN types of human erythrocytes was analysed by SPR as described. The K_D values estimated (by equilibrium analysis) for the interactions with MM and MN Glycophorin A were ~ 0.28 µM and ~0.21 µM respectively, indicating a small (x 1.3-fold) but perhaps significant difference in the affinity of *Pf*EBA175 FL for the Glycophorin A variants (Figure 22). The M variant of Glycophorin A differs from the N variant at two amino acid residues. M is proposed to be ancestral to N in comparison with chimpanzee and orangutan sequences and has serine and glycine at positions 1 and 5 respectively (Ko *et al*., 2011). N on the other hand is characterised by leucine and glutamic acid at these positions. The non-synonomous single nucleotide polymorphisms (SNPs) that give rise to the M and N genotypes are located within the exon 2 of the Glycophorin A gene, GYPA. Interestingly, a recent comparative study of more than 200 GYPA sequences from

ethnically and geographically diverse African populations identified that polymorphisms in exon 2 are under significant balancing selection in individuals in malaria hyper-endemic regions (Ko *et al*., 2011). This finding suggests that the extracellular region of Glycophorin A encoded by exon 2, (containing amino acids 1-25), may play an important role in *P. falciparum* infection. From the observed difference in the affinity of *Pf*EBA175 FL for MM and MN Glycophorin A, it could be postulated that this region of Glycophorin A is directly involved in *Pf*EBA175 FL binding. It further suggests that even polymorphisms in residues that are not sialylated, in this Glycophorin A region, can influence its interaction with *Pf*EBA175 FL. This is consistent with the early observation that *Pf*EBA175 recognition of Glycophorin A is dependent on both the presence of sialic acid and also the sequence of the peptide backbone (Sim *et al*., 1994).

3.3.4 *Pf*EBA175 FL binds to native Glycophorin A with a ~10-fold higher affinity than *Pf*EBA175 RII.

To investigate the binding of *Pf*EBA175 RII to native Glycophorin A, this region of the *Pf*EBA175 extracellular domain was also expressed recombinantly in this study using the mammalian expression system. Denaturing SDS-PAGE analysis of recombinant *Pf*EBA175 RII, after purification of the protein from the culture supernatant by affinity chromatography, revealed that it was expressed at the expected size (Figure 23 D). The protein was found to be primarily monomeric by gel filtration (Figure 23 E). The reference-subtracted sensorgrams obtained by analysing the interaction between *Pf*EBA175 RII and native Glycophorin A, by SPR, were also ‘biphasic’ (Figure 23 F). These sensorgrams thus fitted more closely to a ‘two-state reaction’ kinetic model than to a ‘1:1 binding’ kinetic model, as seen with *Pf*EBA175 FL (Figure 24 B). The data for *Pf*EBA175 RII recognition of Glycophorin A is hence, also consistent with the ‘ligand-induced dimerisation’ model proposed for this interaction.

The K_D values estimated (by equilibrium analysis) for the binding of *Pf*EBA175 RII to MM and MN types of native Glycophorin A were ~2.6 µM and ~2.0 µM respectively, again indicating a x 1.3-fold difference in the affinity of *Pf*EBA175 for the Glycophorin A variants (Figure 24 C). These values also show that the affinity of *Pf*EBA175 RII for native Glycophorin A is ~x 10-fold lower than that of *Pf*EBA175 FL. This may be due to some role played by extracellular regions of *Pf*EBA175 outside of RII to facilitate binding to the erythrocyte receptor and suggests that *Pf*EBA175 FL may be a better vaccine antigen than RII alone.

3.3.5 Functional activity of the extracellular domain of Glycophorin A may be dependent on factors other than sialylation.

To potentially map the *Pf*EBA175 binding site on Glycophorin A, the full-length ectodomain of human Glycophorin A was recombinantly expressed in this study. The recombinant protein was observed to be soluble, glycosylated and immunologically active (Figure 15 A and C). Probing the glycan composition of recombinant Glycophorin A using lectins of known specificity, revealed that it was however under-sialylated in comparison to the native protein (Figure 15 E). Analysis by both AVEXIS and SPR, indicated no recognition of recombinant Glycophorin A by *Pf*EBA175 FL, indicating that the former is non-functional (Figures 16 and 17 E). Co-expression of Glycophorin A with sialyltransferases and a sialic acid transporter increased its level of sialylation (Figure 17 B), but did not confer binding to *Pf*EBA175 FL (data not shown). The lack of any detectable binding of recombinant Glycophorin A to *Pf*EBA175 FL, despite the presence of some α-2,3-linked sialic acid suggests that the activity of the former is perhaps dependent on one/more unknown factor/s in addition to sialylation. For instance, several lines of evidence point to a close association between native Glycophorin A and Band 3 during biosynthesis in erythrocytes (Hassoun *et al*., 1998; Auffray, 2001). Indeed, in Band 3-null mice erythrocytes,

Glycophorin A has been observed to be rapidly degraded in the cytoplasm (Hassoun *et al*., 1998). This has led to the suggestion that Band 3 may perform a chaperone-like role for Glycophorin A. Therefore, it is possible that when the extracellular domain of Glycophorin A is recombinantly-expressed in the absence of Band 3, its conformation deviates from that of the native protein, resulting in inactivity.

3.4 CONCLUSION

In this study, the full-length ectodomain of *P. falciparum* EBA175 (*Pf*EBA175 FL) was expressed in soluble recombinant form using a mammalian expression system and confirmed to be functionally similar to native *P. falciparum* EBA175 from parasite cultures. The recombinantly-expressed protein was shown to bind to native Glycophorin A from MN erythrocytes with a x 1.3-fold higher affinity than to that from MM erythrocytes. Whether this difference in the affinity for M and N Glycophorin A variants would directly influence the efficiency of erythrocyte invasion by *P. falciparum* is not known and should be investigated. Recombinant *Pf*EBA175 FL was also observed to bind native Glycophorin A with a ~10-fold higher affinity than *Pf*EBA175 RII, suggesting some role played by the extracellular regions outside of RII to facilitate binding. *Pf*EBA175 FL could also potentially be a better vaccine candidate than *Pf*EBA175 RII. *Pf*EBA175 FL may be more immunogenic than *Pf*EBA175 RII, due to its larger size and antibodies raised against the different regions of the *Pf*EBA175 FL extracellular domain may act in a synergistic manner to inhibit erythrocyte invasion. Polyclonal antibodies should therefore be raised against each of these antigens and directly compared for inhibition of erythrocyte entry by *P. falciparum*.

3.5 BIBLIOGRAPHY

Adams, J. H., Sim, B. K., Dolan, S. A., Fang, X., Kaslow, D. C. & Miller, L. H. (1992). A family of erythrocyte binding proteins of malaria parasites. *Proceedings of the National Academy of Sciences of the United States of America*, *89*(15), 7085-9.

Auffray, I. (2001). Glycophorin A dimerization and band 3 interaction during erythroid membrane biogenesis: *in vivo* studies in human glycophorin A transgenic mice. *Blood*, *97*(9), 2872-2878.

Batchelor, J. D., Zahm, J. A. & Tolia, N. H. (2012). Dimerisation of *Plasmodium vivax* DBP is induced upon receptor binding and drives recognition of DARC. *Nature Structural Molecular Biology*, *18*(3), 908-914.

Bharara, R., Singh, S., Pattnaik, P., Chitnis, C. E., & Sharma, A. (2004). Structural analogs of sialic acid interfere with the binding of erythrocyte binding antigen-175 to glycophorin A, an interaction crucial for erythrocyte invasion by *Plasmodium falciparum*. *Molecular and Biochemical Parasitology*, *138*(1), 123-9.

Camus, D., & Hadley, T. J. (1985). A *Plasmodium falciparum* antigen that binds to host erythrocytes and merozoites. *Science*, *230*(4725), 553-556.

Chasis JA and Mohandas N. (1992). Red blood cell glycophorins. *Blood*, *80*, 1869-1879.

Chitlaru, T., Kronman, C., Zeevi, M., Kam, M., Harel, A., Ordentlich, A., Velan, B., *et al*. (1998). Modulation of circulatory residence of recombinant acetylcholinesterase through biochemical or genetic manipulation of sialylation levels. *The Biochemical Journal*, *336*, 647-58.

Duraisingh, M. T., Maier, A. G., Triglia, T., & Cowman, A. F. (2003). Erythrocyte-binding antigen 175 mediates invasion in *Plasmodium falciparum* utilizing sialic acid-dependent and -independent pathways. *Proceedings of the National Academy of Sciences of the United States of America*, *100*(8), 4796-801.

El Sahly, H. M., Patel, S. M., Atmar, R. L., Lanford, T. a, Dube, T., Thompson, D., Sim, B. K. L., *et al*. (2010). Safety and immunogenicity of a recombinant nonglycosylated erythrocyte binding antigen 175 Region II malaria vaccine in healthy adults living in an area where malaria is not endemic. *Clinical and Vaccine Immunology*, *17*(10), 1552-9.

Gowda, D. C., & Davidson, E. A. (1999). Protein glycosylation in the malaria parasite. *Parasitology Today (Personal ed.)*, *15*(4), 147-52.

Gu, X., & Wang, D. I. (1998). Improvement of interferon-gamma sialylation in Chinese hamster ovary cell culture by feeding of N-acetylmannosamine. *Biotechnology and Bioengineering, 58*(6), 642-8.

Hassoun, H., Hanada, T., Lutchman, M., Sahr, K. E., Palek, J., Hanspal, M., & Chishti, A. H. (1998). Complete deficiency of glycophorin A in red blood cells from mice with targeted inactivation of the band 3 (AE1) gene. *Blood, 91*(6), 2146-51.

Hossler, P., Khattak, S. F., & Li, Z. J. (2009). Optimal and consistent protein glycosylation in mammalian cell culture. *Glycobiology, 19*(9), 936-49.

Jiang, L., Gaur, D., Mu, J., Zhou, H., Long, C. A., & Miller, L. H. (2011). Evidence for erythrocyte-binding antigen 175 as a component of a ligand-blocking blood-stage malaria vaccine. *Proceedings of the National Academy of Sciences of the United States of America, 108*(18), 7553-8.

Ko, W.-Y., Kaercher, K. A., Giombini, E., Marcatili, P., Froment, A., Ibrahim, M., Lema, G., *et al*. (2011). Effects of natural selection and gene conversion on the evolution of human glycophorins coding for MNS blood polymorphisms in malaria-endemic African populations. *American Journal of Human Genetics, 88*(6), 741-54.

Lopaticki, S., Maier, A. G., Thompson, J., Wilson, D. W., Tham, W.-H., Triglia, T., Gout, A., *et al*. (2011). Reticulocyte and erythrocyte binding-like proteins function cooperatively in invasion of human erythrocytes by malaria parasites. *Infection and Immunity, 79*(3), 1107-17.

Mackenzie, K. R., Prestegard, J. H., & Engelman, D. M. (1997). A Transmembrane Helix Dimer: Structure and Implications. *Science, 276*(5309), 131-133.

Narum, D. L., Haynes, J. D., Fuhrmann, S., Liang, H., Hoffman, S. L., Sim, B. K. L., Moch, K., *et al*. (2000). Antibodies against the *Plasmodium falciparum* receptor binding domain of EBA-175 block invasion pathways that do not involve sialic acids. *Infection and Immunity, 68*(4), 1964-6.

Ockenhouse, C. F., Barbosa, A., Blackall, D. P., Murphy, C. I., Kashala, O., Dutta, S., Lanar, D. E., *et al*. (2001). Sialic acid-dependent binding of baculovirus-expressed recombinant antigens from *Plasmodium falciparum* EBA-175 to Glycophorin A. *Molecular and Biochemical Parasitology, 113*(1), 9-21.

Orlandi, P. A., Klotz, F. W., Haynes, J. D., & Reed, W. (1992). A malaria invasion receptor, the 175-kilodalton erythrocyte binding antigen of *Plasmodium falciparum* recognizes the terminal Neu5Ac (alpha 2-3) Gal- sequences of glycophorin A. *The Journal of Cell Biology, 116*(4), 901-9.

Orlandi, P., Sim, B. K. L., & Chulay, J. (1990). Characterization of the 175-kilodalton erythrocyte binding antigen of *Plasmodium falciparum*. *Molecular and Biochemical Parasitology, 40*, 285-294.

O'Donnell, R. A., Hackett, F., Howell, S. A., Treeck, M., Struck, N., Krnajski, Z., Withers-Martinez, C., *et al*. (2006). Intramembrane proteolysis mediates shedding of a key adhesin during erythrocyte invasion by the malaria parasite. *The Journal of Cell Biology, 174*(7), 1023-33.

Pandey, K. C., Singh, S., Pattnaik, P., Pillai, C. R., Pillai, U., Lynn, A., Jain, S. K., *et al*. (2002). Bacterially expressed and refolded receptor binding domain of *Plasmodium falciparum* EBA-175 elicits invasion inhibitory antibodies. *Molecular and Biochemical Parasitology, 123*(1), 23-33.

Sim, A. B. K. L., Chitnis, C. E., Wasniowska, K., Hadley, T. J., & Miller, L. H. (1994). Receptor and ligand domains for invasion of erythrocytes by *Plasmodium falciparum*. *Science, 264*(5167), 1941-1944.

Sim, B. K. L., Narum, D. L., Chattopadhyay, R., Ahumada, A., Haynes, J. D., Fuhrmann, S. R., Wingard, J. N., *et al*. (2011). Delineation of stage specific expression of *Plasmodium falciparum* EBA-175 by biologically functional region II monoclonal antibodies. *PloS One, 6*(4), e18393.

Tolia, N. H., Enemark, E. J., Sim, B. K. L., & Joshua-Tor, L. (2005). Structural basis for the EBA-175 erythrocyte invasion pathway of the malaria parasite *Plasmodium falciparum*. *Cell, 122*(2), 183-93.

Tomita, M., & Marchesi, V. T. (1975). Amino-acid sequence and oligosaccharide attachment sites of human erythrocyte glycophorin. *Proceedings of the National Academy of Sciences, 72*(8), 2964-68.

van der Merwe, A.P. (2011) Surface Plasmon Resonance in Protein-Ligand interactions: hydrodynamics and calorimetry, edited by S Harding and P Z Chowdhry. *Practical Approach Series, Oxford University Press*, 137-170.

Weikert, S., Papac, D., Briggs, J., Cowfer, D., Tom, S., Gawlitzek, M., Lofgren, J., *et al*. (1999). Engineering Chinese hamster ovary cells to maximize sialic acid content of recombinant glycoproteins. *Nature Biotechnology, 17*(11), 1116-21.

Withers-Martinez, C., Haire, L. F., Hackett, F., Walker, P. A, Howell, S. A, Smerdon, S. J., Dodson, G. G., *et al*. (2008). Malarial EBA-175 region VI crystallographic structure reveals a KIX-like binding interface. *Journal of Molecular Biology, 375*(3), 773-81.

Wong, N. S. C., Yap, M. G. S., & Wang, D. I. C. (2006). Enhancing Recombinant Glycoprotein Sialylation Through CMP-Sialic Acid Transporter Over Expression in Chinese Hamster Ovary Cells. *Biotechnology and Bioengineering*, *93*(5), 1005-16.

Zhang, D., & Pan, W. (2005). Evaluation of three *Pichia pastoris*-expressed *Plasmodium falciparum* merozoite proteins as a combination vaccine against infection with blood-stage parasites. *Infection and Immunity*, *73*(10), 6530-36.